

Rowan University

Rowan Digital Works

Theses and Dissertations

2-14-2018

Preparation of polymeric materials from bio-renewable sources

Jason Douglas Smith
Rowan University

Follow this and additional works at: <https://rdw.rowan.edu/etd>



Part of the [Medicinal-Pharmaceutical Chemistry Commons](#)

Recommended Citation

Smith, Jason Douglas, "Preparation of polymeric materials from bio-renewable sources" (2018). *Theses and Dissertations*. 2518.

<https://rdw.rowan.edu/etd/2518>

This Thesis is brought to you for free and open access by Rowan Digital Works. It has been accepted for inclusion in Theses and Dissertations by an authorized administrator of Rowan Digital Works. For more information, please contact graduateresearch@rowan.edu.

**PREPARATION OF POLYMERIC MATERIALS FROM BIO-RENEWABLE
SOURCES**

by

Jason Douglas Smith

A Thesis

Submitted to the
Department of Chemistry & Biochemistry
College of Science & Mathematics
In partial fulfillment of the requirement
For the degree of
Master of Science in Pharmaceutical Sciences
at
Rowan University
April 20, 2017

Thesis Chair: Subash Jonnalagadda, Ph.D.

© 2018 Jason D. Smith

Dedication

I would like to dedicate this manuscript to my friends and family for always being a constant source of encouragement, laughter, and love. Thank you, from the bottom of my heart. To Kyle, thank you for always being my shoulder to cry on, my biggest fan, my foundation; words cannot express how much I love you.

Acknowledgments

I would like to acknowledge and thank Dr. Subash Jonnalagadda, my thesis chair and advisor, as well as, Dr. Joseph F. Stanzione III, Dr. Kandalam Ramanujachary, and Dr. Amos Mugweru, faculty collaborators on this project and its roots. Additionally, I would like to thank Dr. Suman Pathi, our research group's post-doctoral research associate. I would also like to thank my fellow master's students within my research group, Agasthya Kasibotla, Bhawan Patel, and Keyur Pandya. I would be remiss if I did not also thank the Department of Chemistry and Biochemistry at Rowan University and the University in its entirety for providing me with a research fellowship during my time within this program.

Abstract

Jason D. Smith

PREPARATION OF POLYMERIC MATERIALS FROM BIO-RENEWABLE
SOURCES
2017-2018

Subash Jonnalagadda, Ph.D.

Master of Science in Pharmaceutical Sciences

The focus of this project was to develop methodologies for the preparation of novel polymeric materials from bio-renewable sources. In order to complete this task we needed (a) unfettered access to bio-based materials and ways to convert them to value needed chemicals, as well as, (b) reaction protocols that would allow greater diversity during the synthesis of polymeric compounds so as to affect the properties of these materials.

Our research group has a background in converting plant-based materials like cellulose into value added chemicals employing catalytic reactions. The polymerization of these monomers was then conducted utilizing the Baylis-Hillman reaction. The resulting alcohol adduct obtained from this reaction allowed for various alterations on the polymer with relative ease. This chemical versatility of the Baylis-Hillman reaction offers tremendous potential toward the synthesis of an array of polymeric materials.

Table of Contents

Abstract.....	v
List of Figures.....	viii
Chapter 1: Introduction.....	1
Betulin.....	1
Extraction and Purification of Betulin.....	1
Synthesis of Betulin Derivatives.....	2
Introduction to Polymers.....	2
Advantages of Polymer-Based Drug Delivery Systems.....	3
Polymer Arrangements & Classifications.....	4
Biomass in Polymer Chemistry.....	5
Utilization and Advantages.....	5
Biomass Polymerization Cycle.....	6
Previous Research.....	8
Synthesis of Mesoporous Zirconium Phosphate.....	10
Synthesis of 5-Hydroxymethyl-2-furfural.....	11
Synthesis of Furan-2,5-dicarboxylic Acid.....	11
Synthesis of Spinel $\text{Li}_2\text{CoMn}_3\text{O}_8$ Catalyst.....	12
Synthesis of Furan-2,5-dicarboxylic Acid.....	13
Multi-Component Coupling Reactions.....	14
Passerini Reaction.....	15
The Ugi Reaction.....	16

Table of Contents (Continued)

The Baylis-Hillman Reaction	19
Discovery and Advantages	19
Reaction Mechanism.....	20
Scope of the Reaction	24
Chapter 2: Synthesis of Polymers	28
Williamson Ether Synthesis.....	28
Esterification	29
Reduction of an Aldehyde to a Primary Alcohol.....	30
Conversion of Allylic Alcohols to Allyl Bromides	30
Vanillin-Derived Methacrylate Polymers	31
Reaction Scheme.....	31
4-Hydroxybenzaldehyde-Derived Methacrylate Polymers.....	33
Reaction Scheme.....	33
Vanillin-Derived Bisacrylate Polymers	35
Reaction Scheme.....	35
Terephthaldehyde-Derived Bisacrylate Polymers	38
Reaction Scheme.....	38
Alternate Polymerization Reactions	40
Reaction Scheme.....	40
Chapter 3: Data	44
Identification & Characterization	44
References.....	66

List of Figures

Figure	Page
Figure 1. The triterpene, Betulin.....	1
Figure 2. Betulin-28-Succinate.	2
Figure 3. Polymer Arrangements: Block Copolymer, Graft Copolymer,.....	4
Figure 4. A number of the various possible sources of readily available biomass.	6
Figure 5. The biomass polymerization cycle.	7
Figure 6. Synthesis of furan-2,5-dicarboxylic acid from biomass derived compounds ..	8
Figure 7. The Strecker reaction.....	14
Figure 8. The resonance structures of C-IV and C-II of isocyanide.....	15
Figure 9. Reaction mechanism of the Passerini reaction.	16
Figure 10. Reaction sequence of the Ugi reaction.	17
Figure 11. Proposed reaction mechanism of the Ugi reaction.	18
Figure 12. The Baylis-Hillman reaction.	19
Figure 13. The initial proposed Baylis-Hillman reaction mechanism.	20
Figure 14. Reaction Mechanism of McQuade.	22
Figure 15. Alcohol-catalyzed Reaction Mechanism of Aggarwal.....	23
Figure 16. Simplified reaction mechanism for the Baylis-Hillman reaction.	24
Figure 17. Versatility of the activated alkene within the Baylis-Hillman reaction.	25

List of Figures (Continued)

Figure	Page
Figure 18. Dimerization of the alkene in the presence of a poor electrophile.....	25
Figure 19. Common Baylis-Hillman catalysts.....	26
Figure 20. Reaction sequence of the Williamson ether synthesis.....	28
Figure 21. Mechanism of the formation of epoxide from 2-chloroethanol.	29
Figure 22. Secondary reaction of phenolic compounds reacting with formed epoxides	29
Figure 23. Esterification.....	29
Figure 24. Reaction mechanism for the reduction of an aldehyde to a primary alcohol	30
Figure 25. Conversion of an allylic alcohol to an allyl bromide.	31
Figure 26. Vanillin-derived methacrylate polymers.	32
Figure 27. 4-Hydroxybenzaldehyde methacrylate polymers.	34
Figure 28. Vanillin-derived bisacrylate polymers.	36
Figure 29. Synthesis of terephthaldehyde-derived bisacrylate polymers.	38
Figure 30. Reaction scheme of terephthaldehyde/methacrylate & piperazine polymers.	40
Figure 31. Reaction scheme of terephthaldehyde & piperazine based polymers.	42
Figure 32. 400 MHz ¹ H NMR of Compound 1 in CDCl ₃	44
Figure 33. 400 MHz ¹ H NMR of Compound 2 in CDCl ₃	45
Figure 34. GPC Spectrum of Compound 3	46

List of Figures (Continued)

Figure	Page
Figure 35. 400 MHz ^1H NMR of Compound 4 in CDCl_3	47
Figure 36. 400 MHz ^1H NMR of Compound 5 in CDCl_3	48
Figure 37. GPC Spectrum of Compound 6	49
Figure 38. 400 MHz ^1H NMR of Compound 7 in $\text{DMSO} - d_6$	50
Figure 39. 400 MHz ^1H NMR of Compound 8 in $\text{DMSO} - d_6$	51
Figure 40. GPC Spectrum of Compound 9	52
Figure 41. 400 MHz ^1H NMR of Compound 10 in CDCl_3	53
Figure 42. 400 MHz ^1H NMR of Compound 11 in CDCl_3	54
Figure 43. 400 MHz ^1H NMR of Compound 12 in CDCl_3	55
Figure 44. 400 MHz ^1H NMR of Compound 13 in CDCl_3	56
Figure 45. 400 MHz ^1H NMR of Compound 14 in CDCl_3	57
Figure 46. 101 MHz ^{13}C NMR of Compound 14 in CDCl_3	58
Figure 47. MS Analysis for Compound 14	59
Figure 48. IR Spectrum of Compound 14	60
Figure 49. 400 MHz ^1H NMR of Compound 16 in CDCl_3	61
Figure 50. 400 MHz ^1H NMR of Compound 17 in CDCl_3	62
Figure 51. 101 MHz ^{13}C NMR of Compound 17 in CDCl_3	63

List of Figures (Continued)

Figure	Page
Figure 52. MS Analysis for Compound 17	64
Figure 53. IR Spectrum of Compound 17	65

Chapter 1

Introduction

Betulin

Betulin is a naturally occurring triterpene found often in the bark of stem of trees. In some instances it can make up to 30% of the dried weight of the bark of birch trees.¹ Its derivatives have shown extensive pharmacological activity as potential antimalarial, anti-inflammatory, and anti-HIV agents. It has also shown activity against several varieties of tumor cell lines.¹ The major issue associated with betulin, however, is its aqueous solubility.

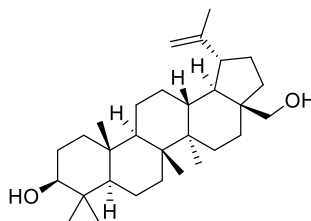


Figure 1. The triterpene, Betulin

Extraction and purification of betulin. Prior to the chemical manipulations of betulin, we extracted and purified the natural product from one of its most prevalent sources, the bark of the birch tree. Our initial methods consisted of extracting the compound by shredding the bark into thin strips and refluxing them in chloroform for 2-3 hours. The next step involved filtering the resulting solution via suction filtration and allowing the resulting compound to recrystallize in an ice bath. This method yielded

anywhere from 15-30% betulin. While the yield was satisfactory, additional recrystallizations and column chromatography were necessary to increase the purity of the compound prior to further chemical manipulations.¹

Synthesis of betulin derivatives. Once betulin was obtained it was then utilized for organic syntheses. In order to make it more polar, the primary alcohol on C₂₈ was first esterified with succinic anhydride in the presence of 4-(dimethylamino)pyridine (DMAP) in dichloromethane under reflux conditions for five hours.² The resulting compound, betulin-28-succinate (Figure 2) provided a readily available acid to be utilized in known multi-component coupling reactions such as the Passerini and Ugi reactions. Insert reference here.

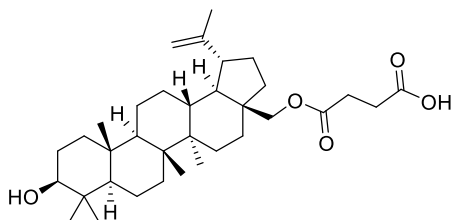


Figure 2. Betulin-28-Succinate.

Introduction to Polymers

A polymer is a chemical compound consisting of a number of repeating units bonded together to form a new compound. Often times these polymers have many types of

uses including applications as plastics or resins. Additionally, polymers also have the ability to act as controlled carriers for low molecular weight drugs. These types of polymers allow for increased pharmacokinetics and pharmacodynamics.³

Polymer chemistry has been in development for several decades but its continued growth is evident based on the pharmaceutical market. In 2013, the pharmaceutical market was valued at approximately \$151.3 billion. By 2018, that revenue is estimated at \$173.8 billion. This shows a compound annual growth rate of 2.8%.⁴

Polymers are synthesized utilizing carbon-carbon bond forming reactions in such a manner that the starting unit, or units, are repeated in a way to form a larger chain of said structures. The precursor compounds that make up these polymers are known as monomers.

Advantages of Polymer-Based Drug Delivery Systems

Polymers are unique compared to traditional drug dosage systems. Some of the key advantages of polymer-based drug delivery systems include providing an increased absorption rate and biocompatibility, cell and tissue specific targeting of drugs, the prevention of drug degradation due to bodily enzymes, as well as, control of the drug's concentration in the body over a longer duration within the therapeutic window.⁵ One of the most important characteristics of these polymers however; is the flexibility of their characteristics allowing for production on an industrial scale with a continued availability for additional alterations.⁶

Polymer Arrangements & Classifications

Although certain polymers can affect the rate of dissolution of a compound within the body, not all polymers are alike. Polymers come in three different types of arrangements: block copolymers, graft copolymers, and random copolymers (Figure 3).

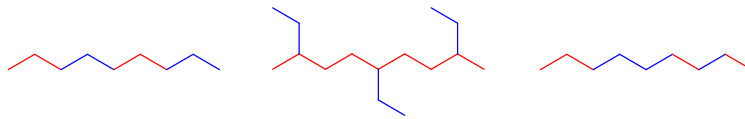


Figure 3. Polymer Arrangements: Block Copolymer, Graft Copolymer, and Random Copolymer.

Block copolymers, consist of one or more repeating monomer units in a specific repeating order. Graft copolymers, consist of a chain of one type of monomer unit with branches of one or more other monomer units. Lastly, random copolymers have repeating monomer units, but in no distinct repetitive pattern; the order of the units is random.⁷

Polymers are also classified based on their origin. The different types of classifications include natural polymers, synthetic polymers, or a combination of both.⁸

Although natural polymers are consistently abundant and biodegradable, they pose significant issues in reproducibility and purification. Synthetic polymers have a higher immunogenicity, which prevents long-term usage. If the polymer itself is non-

biodegradable it also needs to be surgically removed after use.⁹ These disadvantages suggest the need for new polymer candidates that address these concerns. It was in this regard that the associated polymers within this project were designed.

Biomass in Polymer Chemistry

While creating novel polymers for potential applications in drug delivery was a main goal of this project, we wanted to do so while also focusing on the feasibility and affordability of such syntheses. Waste biomass derived from plants and crops provides an alternate, affordable route for the production of chemicals and fuels.¹⁰ This chapter covers the utilization and advantages of biomass in polymer chemistry, the biomass polymerization cycle, as well as, previous research in biomass derived compounds.

Utilization and advantages. Biomass is readily available and it acts as a renewable potential substitute for fossil fuels. The continued use of the products that lead to said waste biomass will occur for years to come, thus providing an unfettered source for the conversion of this biomass into relevant polymer synthesis reactants.¹¹

Biomass is obtained from a variety of sources. These include agricultural and forestry crops and residues. Biomass derived from these areas accounts for roughly 25% of the global requirement. Additional sources include industry residues, sewage, animal residues, and municipal waste to name a few. Annually, the worldwide production of biomass exceeds 100 trillion kilograms.

Despite the fact that overall global production of biomass is substantial in quantity, currently, only about 5% of chemicals are derived from renewable resources.¹² The numerous sources of biomass are listed in Figure 4.

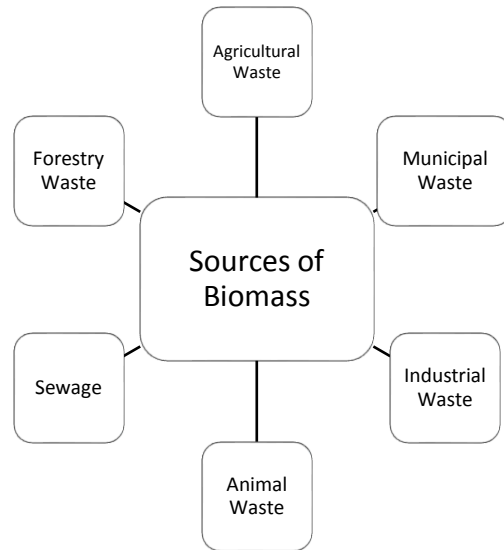


Figure 4. A number of the various possible sources of readily available biomass.

Biomass polymerization cycle. Although there are numerous routes to procuring biomass, these compounds are not useful unless they can be readily converted into value-added compounds. This process begins by understanding the Biomass Polymerization Cycle.

The process begins when carbon dioxide and water in plants utilize sunlight during photosynthesis to synthesize cellulosic materials as useful cultivated crops. This is a

primary source of edible biomass that is derived from harvesting the grown vegetation. The non-edible waste that results from the manufacture of these food items are equally beneficial to our society and our overall wellbeing. By utilizing solvents and various aromatics we can isolate key known compounds from this biomass waste such as, cellulose, hemicellulose, and lignin. These compounds can then undergo various catalytic reactions to yield value-added chemicals derived from biomass. By performing various organic reactions these monomeric value-added chemicals can be transformed into polymers and as these polymers are biomass-based they could potentially be biodegradable to generate carbon dioxide and water, thus restarting the biomass polymerization cycle (Figure 5).

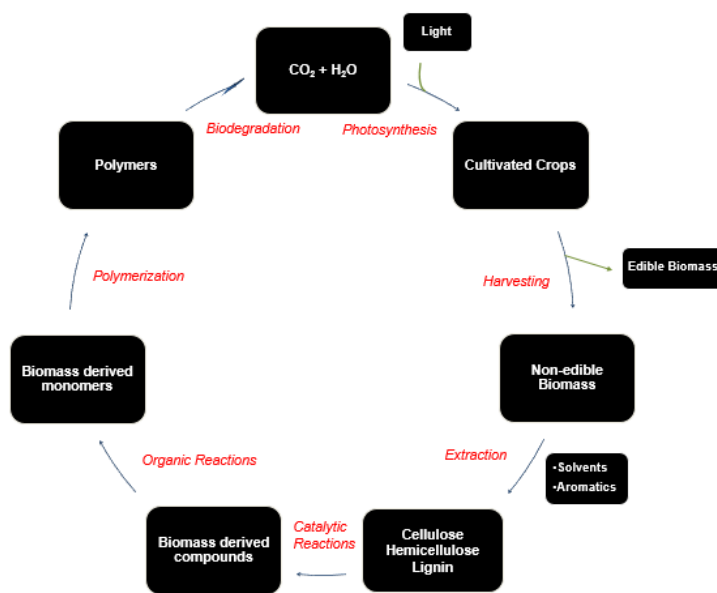


Figure 5. The biomass polymerization cycle.

Previous Research

Previously, our group had reported the conversion of carbohydrates such as fructose, glucose, and sucrose into a chemical called 5-hydroxymethyl-2-furfural, and subsequent conversion to furan-2,5-dicarboxylic acid (Figure 6).

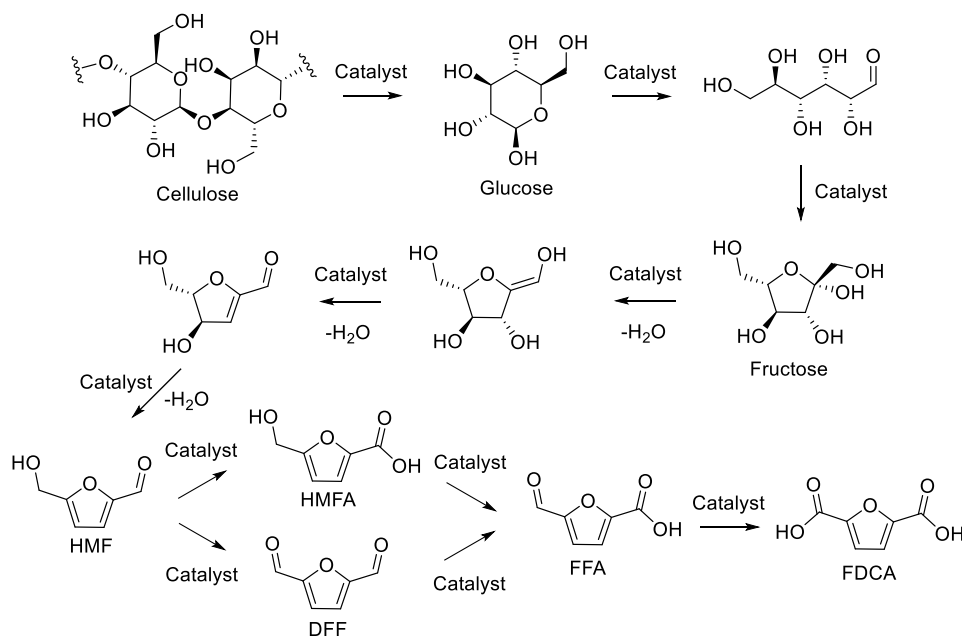


Figure 6. Synthesis of furan-2,5-dicarboxylic acid from biomass derived compounds.¹¹

The synthesis of furan-2,5-dicarboxylic acid offers a substitute for terephthalic acid. Terephthalic acid is currently utilized in the polymer industry as a precursor to polyethylene terephthalate, commonly known as PET. Terephthalic acid is derived from

fossil fuels, therefore finding a meaningful biomass-derived substitute could have a profound impact on the industry.¹¹

To synthesize furan-2,5-dicarboxylic acid our research group first had to synthesize a relevant precursor compound, 5-hydroxymethyl-2-furfural. Glucose proved to be the most effective of the biomass derived compounds. Synthesizing 5-hydroxymethyl-2-furfural from glucose, however, first required isomerization to fructose.¹¹

Various catalysts have been evaluated to improve the yields of 5-hydroxymethyl-2-furfural synthesis from metal chlorides to heterogeneous catalysts like zeolites, ion-exchange resins, heteropoly acid salts, sulfated and phosphoric acid-treated metal oxides, and more. Changes in solvent systems have also been evaluated for potential improvements in yield. These have included ionic liquids and aqueous/bi/multiphase organic solvent systems. Metal phosphates, including aluminum, titanium, zirconium, and niobium have also been evaluated as heterogeneous acid catalysts to convert sugars into 5-hydroxymethyl-2-furfural.insert reference here.

This process is possible due to the duality of the Lewis and Brønsted acidic sites present within the catalyst. The metal sites within the catalyst act as Lewis acidic sites while the protonated phosphate groups act as Brønsted acidic sites. Research has found that the Lewis acidic sites of the catalyst provide for enhanced isomerization of glucose to fructose via an intermolecular hydride shift. Concurrently, the Brønsted acidic sites allow for, and assist with, the dehydration of fructose to 5-hydroxymethyl-2-furfural.¹¹

Synthesis of mesoporous zirconium phosphate. Our group began by focusing on mesoporous zirconium phosphate (ZrP) as a potential catalyst. The synthesis involved hydrothermal treatment with an in situ generated zirconium carbonate complex, di-ammonium hydrogen orthophosphate and hexadecyl trimethyl ammonium bromide (CTAB) in a basic medium. CTAB being a micelle-forming agent allowed for porosity in the catalyst. White zirconium carbonate was precipitated out of the mixture by mixing with dilute aqueous solutions of ammonium carbonate and zirconium oxychloride while stirring. Once the precipitation reaction had completed it was collected through centrifugation and repeated washings with water to remove traces of chloride ions. The chloride-free precipitate was then mixed with an aqueous solution of ammonium carbonate and stirred vigorously until a clear solution was obtained. This solution was then diluted to 175.0 mL using distilled water. A 50.0 mL aqueous solution of 6.5506 g di-ammonium hydrogen orthophosphate was added to the clear solution at a fixed rate of 5.0 mL min⁻¹ to make a 225 mL solution of 1.0 % (w/v). The aqueous solutions containing CTAB were then placed in a 1000.0 mL thick-wall glass bottle and stirred continuously for 12.0 h at room temperature, then at 80.0 °C for 2 days and finally at 90.0 °C for 1 day in the same glass bottle. The reaction was then left for another day in a Teflon-lined stainless steel Parr bomb reactor which was kept in a pre-heated hot air oven at 135.0 °C. Once cooled, the white precipitate was centrifuged, washed with distilled water, and dried in a hot air oven at 80.0 °C for 12.0 h. The dried samples were then calcined in a high-temperature furnace at 550.0 °C for 6 h to obtain pure mesoporous zirconium phosphate. The molar ratio for the synthesis was $Zr^{4+}/PO_4^{3-}/CTAB/H_2O$: 1:2:0.25:1000.¹¹

Synthesis of 5-hydroxymethyl-2-furfural. Reactions were conducted in thick-wall glass pressure tubes. The typical experiment consisting of sugar, catalyst, a saturated NaCl aqueous phase, and diglyme. A 1:3 ratio was utilized for the volumes of aqueous phase and diglyme. The reaction vessel was sealed and placed in a pre-heated oil bath at a set temperature with continuous stirring. After the allotted time the reaction was cooled down in an ice bath and transferred to a centrifuge tube. The mixture was separated from the catalyst through centrifugation. The catalyst was washed with water and acetone and dried in a hot air oven at 100.0 °C. The liquid layer underwent analysis through high-performance liquid chromatography. The mobile phase consisted of acidic water and methanol (0.05% H₂SO₄ (10%) + MeOH (90%)) at a flow rate of 1.0 mL min⁻¹. 5-hydroxymethyl-2-furfural was identified based off of its retention time compared to the standard sample. The concentration amount determined from the calibration plot. The reaction sequence with the highest yield was based off of starting with a 2:1 ratio of fructose to zirconium phosphate reacting for 1 hour at 150.0 °C resulting in a yield of 80%.¹¹

Synthesis of furan-2,5-dicarboxylic acid. The oxidation of 5-hydroxymethyl-2-furfural to furan-2,5-dicarboxylic acid has been evaluated and tested in a variety of ways including dehydration of hexose, stoichiometric oxidants like metal permanganates, and homogeneous metal salts like cobalt, manganese, and bromine by autoxidation under high pressure. Additional research has focused on catalytic aerobic oxidation using homogeneous catalysts like Co(OAc)₂, Mn(OAc)₂, and HBr in acetic acid but yielded either 2,5-diformyl furan in 57% yield or furan-2,5-dicarboxylic acid in 60% yield dependent upon the oxidation conditions. Oxidation of 5-hydroxymethyl-2-furfural using

$\text{Co}(\text{OCOCH}_3)_2$ and $\text{Mn}(\text{OCOCH}_3)_2$ in a 1:1 ratio in the presence of NaBr resulted in the formation of furan-2,5-dicarboxylic acid in an amount equal to 49% of 5-hydroxymethyl-2-furfural.¹¹

The literature preparation of furan-2,5-dicarboxylic acid from 5-hydroxymethyl-2-furfural involves either heterogeneous catalysis or enzymatic pathways. The former being preferred over homogeneous catalysts due to ease of separation and reuse of the catalyst. Many heterogeneous supported catalysts have been investigated including precious metals like platinum and gold. While their yields were as high as 99% the economic feasibility of an industrial scale application proved impractical. Our group was able to successfully synthesize furan-2,5-dicarboxylic acid from 5-hydroxymethyl-2-furfural with 100% conversion and 80% isolated yield in the presence of a solid catalyst spinel $\text{Li}_2\text{CoMn}_3\text{O}_8$ using molecular oxygen as oxidant under pressure conditions.¹¹

Synthesis of spinel $\text{Li}_2\text{CoMn}_3\text{O}_8$ catalyst. The $\text{Li}_2\text{CoMn}_3\text{O}_8$ catalyst was synthesized using gel-pyrolysis method. This method involves a gel being obtained by heating an acidic solution of metal salts in the presence of urea and citrate at a temperature of 80.0 °C. The gel was then heated at 350.0 °C and subjected to acid treatment for the removal of lithium atoms to yield mixed metal oxide spinel catalyst. The role of urea and citrate in the synthesis controlled the growth of crystals by forming a porous polymeric network. The usual experiment involved an aqueous solution of citric acid monohydrate (34.16 g, 1.63 mmol) and urea (9.76 g, 1.63 mmol) mixed with an aqueous solution of LiNO_3 (1.87 g, 27 mmol), $\text{Mn}(\text{OAc})_2 \cdot 4\text{H}_2\text{O}$ (11.96 g, 48.8 mmol), and $\text{Co}(\text{NO}_3)_2 \cdot 6\text{H}_2\text{O}$ (1.57 g, 5.42 mmol). Concentrated nitric acid (HNO_3) was added to the solution in 10%

v/v ratio. The resulting solution was evaporated at 80.0 °C with continuous stirring to remove any water. The resulting gel was yellowish in color and dried at 170.0 °C for 12 h. The resin that remained was sponge-like and was calcined in air at 350.0 °C for 12 h to yield an ash like black powder. This powder was then subjected to the acid treatment. Concentrated nitric acid was added drop wise to an aqueous suspension of the black powder while stirring continuously until the pH of the solution was approximately 2. Upon completion of the acid treatment the resulting solid was collected by centrifugation and washings with distilled water until the pH of the decanted water was roughly 7. The solid was then dried at 85.0 °C in a hot air oven. The dark brown product was identified as $\text{Li}_2\text{CoMn}_3\text{O}_8$ by powder X-ray diffraction technique.

Synthesis of furan-2,5-dicarboxylic acid. The oxidation reactions were performed in 300.0 mL Teflon-line stainless steel autoclave Parr reactors with pure O_2 gas as an oxidant. The typical reaction contained a mixture of 5-hydroxymethyl-2-furfural (1.0 g, 8.0 mmol), glacial acetic acid/aqueous sodium hydroxide solution (50.0 mL), $\text{Li}_2\text{CoMn}_3\text{O}_8$ (0.205 g, 7.0 mol% *w.r.t* HMF) and sodium bromide (0.027 g, 3.3 mol% *w.r.t* HMF). The parr reactor was placed in the bench-top heater and the temperature raised. The oxygen gas was then slowly added into the reactor. A sample (0.5 mL) of the product solution was obtained, by removing the head of the reactor and then filtered using a 0.2 μm PTFE filter. Analyses of the sample products were performed utilizing high performance liquid chromatography with a UV detector. The mobile phase consisting of acidic water and methanol (0.05% H_2SO_4 (10.0%) + MeOH (90.0%)) at a flow rate of 1.0 mL min^{-1} . The

product was identified by retention times compared with standard samples. Further isolation and purification was also conducted.¹¹

Successful means of synthesizing the monomeric compound furan-2,5-dicarboxylic acid from biomass derived compounds allows for direct applications of this project to have real-world applications in future applications and research.

Multi-Component Coupling Reactions

Our group has been working on the development of novel methodologies for the synthesis of various chemical motifs utilizing multi-component coupling reactions such as the Passerini and Ugi reactions.

Multi-component coupling reactions are reactions that involve more than two reactants combining in such a manner so as to produce one highly selective product that retains a majority of the starting reactants.¹² The first documented multi-component coupling reaction was the Strecker synthesis of α -amino cyanides in 1850 from which α -amino acids were synthesized (Figure 7).

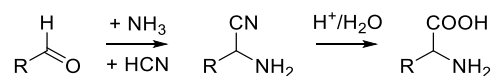


Figure 7. The Strecker reaction.

Today, however, a wide range of multi-component coupling reactions exist. Of the multi-component coupling reactions in existence, isocyanide based multi-component coupling reactions are among the most frequently exploited. This is largely in part due to the functionality of isocyanide. Studies have suggested that the isocyanide is able to exhibit resonance between its tetravalent and divalent carbon structures. This allows for both electrophilic and nucleophilic reactions at the C-II atom which then converts to the C-IV structure in an exothermic reaction (Figure 8).

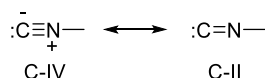


Figure 8. The resonance structures of C-IV and C-II of isocyanide.¹³

Of the many isocyanide derived multi-component coupling reactions, the Passerini and Ugi reactions are the most prominent.

Passerini reaction. The Passerini reaction was discovered by Mario Passerini in Florence, Italy in 1921 and was the first multi-component reaction utilizing isocyanides. It is a simple three component reaction combining a carboxylic acid, aldehyde (or ketone), and isocyanide into an α -acyloxy-carboxamide (Figure 9).¹⁴

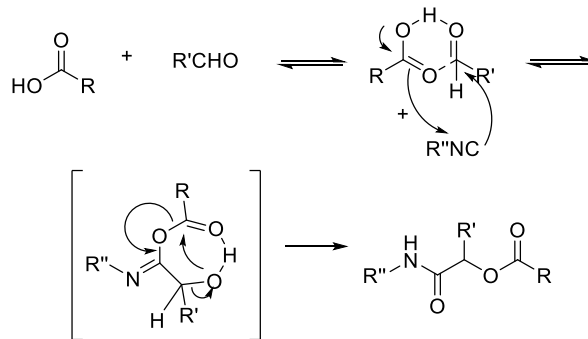


Figure 9. Reaction mechanism of the Passerini reaction.¹⁵

The mechanism for the reaction involves a trimolecular reaction between the isocyanide, carboxylic acid, and carbonyl in a sequence of nucleophilic additions. The transition state consists of a five-membered ring with partial covalent and double bonding. The second step of the reaction consists of an acyl transfer to the neighboring hydroxyl group.

The Passerini reaction has been utilized in a number of reactions including the preparation of polymers from renewable materials.¹⁶

The Ugi reaction. Named after Estonian-born German chemist, Ivar Karl Ugi, the Ugi reaction is another multi-component coupling reaction utilized in organic syntheses that was first reported in 1959. Like the Passerini reaction, the Ugi reaction involves a ketone or aldehyde, an isocyanide, and a carboxylic acid, however, the Ugi reaction also

involves an amine. These organic compounds coalesce exothermically to produce a bis-amide in a one pot synthesis (Figure 10).

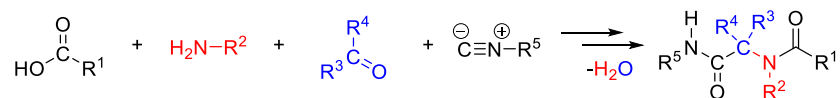


Figure 10. Reaction sequence of the Ugi reaction.

The reaction first involves the formation of an imine from the amine and ketone via the loss of one equivalent of water. This step is then followed by the reaction of the imine with the isocyanide and the carboxylic acid providing the reaction intermediate. The exact mechanism for the formation of the intermediate is not known but one proposed mechanism involves a proton exchange between the carboxylic acid and the previously formed imine resulting in an activated iminium ion susceptible to nucleophilic addition of the isocyanide's terminal carbon atom to the nitrilium ion. It is suggested that this is then followed by a second nucleophilic addition between the intermediate and the carboxylic acid anion. The intermediate then rearranges via a Mumm rearrangement acyl transfer into the final bis-amide. This is the step that drives the reaction to completion as all previous steps are readily reversible (Figure 11).¹⁷

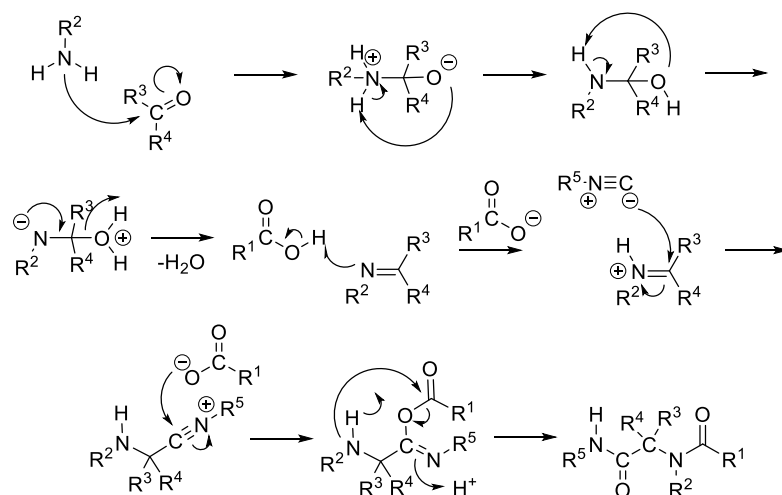


Figure 11. Proposed reaction mechanism of the Ugi reaction.

Due to its versatility, the Ugi reaction was one of the first reaction sequences to be utilized for the creation of chemical libraries. Chemical libraries consist of sets of compounds that can be readily synthesized and tested consistently for comparison and efficacy in various applications.

The concept of chemical libraries consists of utilizing many different starting materials and changing them ever so slightly to produce unique and novel products with relative ease. A reaction consisting of five different ketones, five types of amines, five isocyanides, and five carboxylic acids could theoretically yield 625 different, unique, and novel products simply by following one reaction sequence. This is a direct application of the principles of combinatorial chemistry.

The Baylis-Hillman Reaction

As a precursor test of feasibility we focused on utilizing vanillin and p-hydroxybenzaldehyde as our biomass derived compounds for this project. Both vanillin and p-hydroxybenzaldehyde are readily commercially available at reasonable prices.

Our group has had extensive experience with the Baylis-Hillman reaction in our multitude of projects. We wanted to investigate the potential of this reaction for the formation of polymeric materials.

Discovery and advantages. The Baylis-Hillman reaction is named for British scientist Anthony B. Baylis and German scientist Melville E. D. Hillman. It is a carbon-carbon bond forming reaction between the α -position of an activated alkene and an aldehyde or carbon electrophile. By utilizing a nucleophilic catalyst, such as a tertiary amine or phosphine, the reaction provides a product with high functionality such as an allylic alcohol when aldehyde is used as the electrophile (Figure 12).

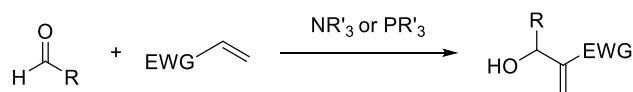


Figure 12. The Baylis-Hillman reaction.

The advantages associated with the Baylis-Hillman reaction include that it is an atom-economic coupling of easily prepared/obtained starting materials, the reaction of a pro-chiral electrophile allows for the generation of a chiral center and applications asymmetric synthesis, its products usually contain multiple functionalities in close proximity which allow for further transformations, as well as, its ability to employ a nucleophilic organo-catalytic system without the use of heavy metals and under relatively mild conditions.¹⁸

Reaction mechanism. The reaction mechanism for the Baylis-Hillman reaction was first proposed by Professor H. M. R. Hoffmann in 1983. His proposed reaction sequence involved a 1,4-addition of the catalytic tertiary amine to the activated alkene to create a zwitterionic aza-enolate followed by its addition to the aldehyde via an aldol addition. The last step then involved an intramolecular proton shift generating the final adduct and releasing the catalyst via E2 or E1cb elimination (Figure 13).

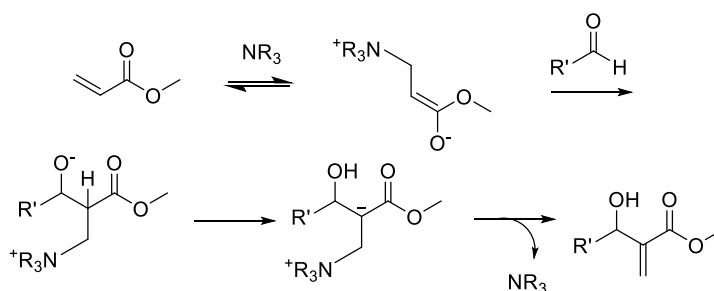


Figure 13. The initial proposed Baylis-Hillman reaction mechanism.

The initial mechanism, however, did not account for several factors later presented. The rate of the reaction was found to have been accelerated by the build-up of product (the autocatalytic effect), the mechanism as proposed was not supported by these findings. Additional reactions involving aryl aldehydes and acrylates also resulted in unique dioxanone byproducts that would not be plausible under the original mechanism. McQuade and Aggarwal began reevaluating the theoretical and kinetic mechanisms with a focus on the proton-transfer step.¹⁹

McQuade began working on methyl acrylate and p-nitrobenzaldehyde as his reactants. He observed that the reaction was second order relative to the aldehyde with significant kinetic isotope effect at the α -position of the acrylate. Regardless of the solvent used, the kinetic isotope effect was found to be greater than 2 indicating a relevancy to the proton abstraction step. This was indicative of the proton abstraction step as the rate determining step. It was with these new findings that McQuade then proposed a new mechanism for the Baylis-Hillman reaction. The first and second steps of the sequence remain the same as the original mechanism by Hoffmann, however after the first aldol addition, McQuade predicted that the subsequent addition of the aldehyde would occur to form a hemiacetal alkoxide instead. The rate determining proton transfer step via a six-membered transition state would then release the adduct which would then react to produce the product or dioxanone byproduct. This mechanism successfully accounted for the formation of dioxanone as a byproduct (Figure 14).²⁰

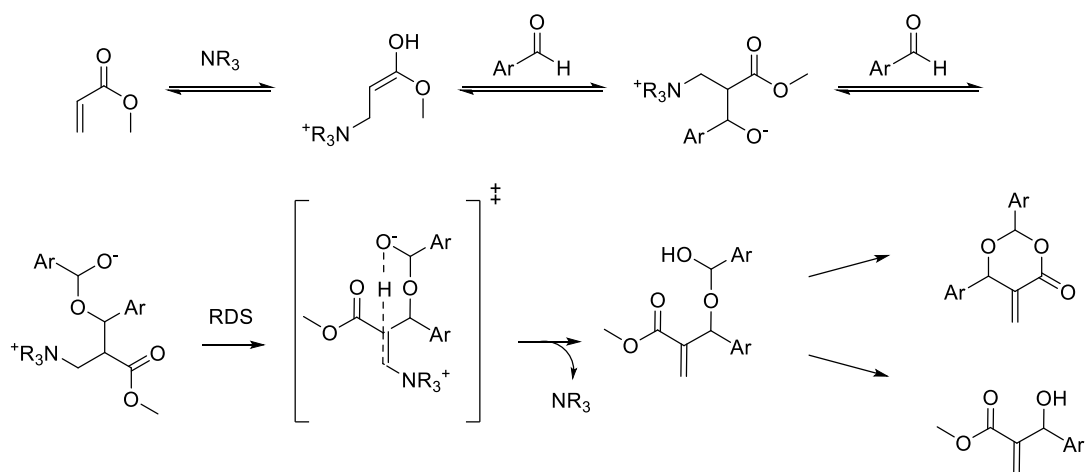


Figure 14. Reaction Mechanism of McQuade.

Aggarwal focused primarily on the autocatalytic effect. He suggested that the early stages of the reaction follow McQuade's suggested mechanism but that after ~20% conversion the alcohol-catalyzed mechanism dominates. He suggested that the accompanying catalytic alcohol assists in the rate-determining proton transfer step via a six membered transition state (Figure 15).

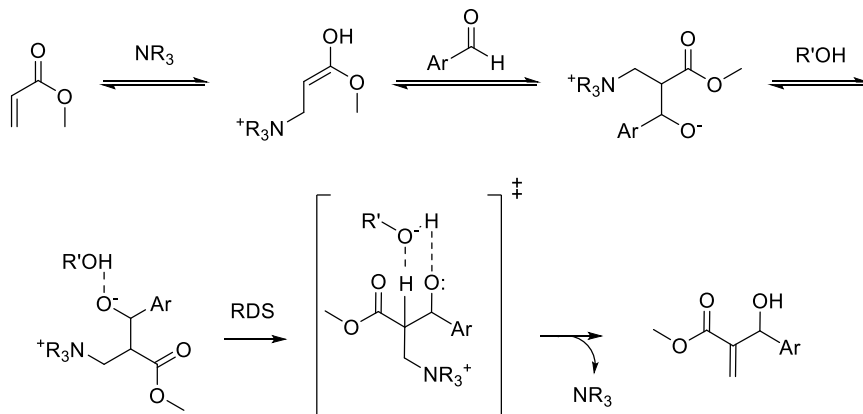


Figure 15. Alcohol-catalyzed Reaction Mechanism of Aggarwal.

While McQuade and Aggarwal's publications answered a number of the underlying questions related to the mechanism of the Baylis Hillman reaction there were still a number of unanswered mysteries regarding the reaction, including clarifying the role of the intermediate. The commonly accepted and simplified mechanism for the Baylis-Hillman reaction today involves the Michael addition of the nucleophilic catalyst to the activated alkene followed by quenching the zwitterionic adduct with the electrophile via Aldol condensation and a proton transfer and elimination of the catalyst (Figure 16).

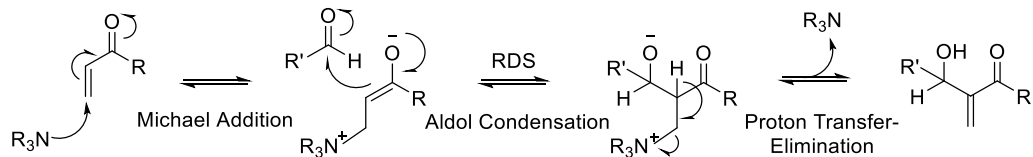


Figure 16. Simplified reaction mechanism for the Baylis-Hillman reaction.

Scope of the reaction. The scope of the Baylis-Hillman reaction is dependent upon a multitude of factors including the alkene and its versatility, the selection of the electrophile being used, as well as the type of catalyst being used.

Alkene versatility. The Baylis-Hillman reaction allows for a wide range of activated alkenes within the reaction mechanism. The ambient conditions employed in the Baylis-Hillman reaction increases the versatility of the potential alkenes that can be utilized in this reaction. The only time changes in pressure are required are when hindered β -substituted derivatives are present within the system requiring an increase in pressure to react. When hydrogen bonding is present within the alkene it increases the rate of the reaction due to the stabilization of the adduct and/or activation of the aldehyde. There is a multitude of Baylis-Hillman products possible simply by utilizing a large variety of activated alkenes (Figure 17).

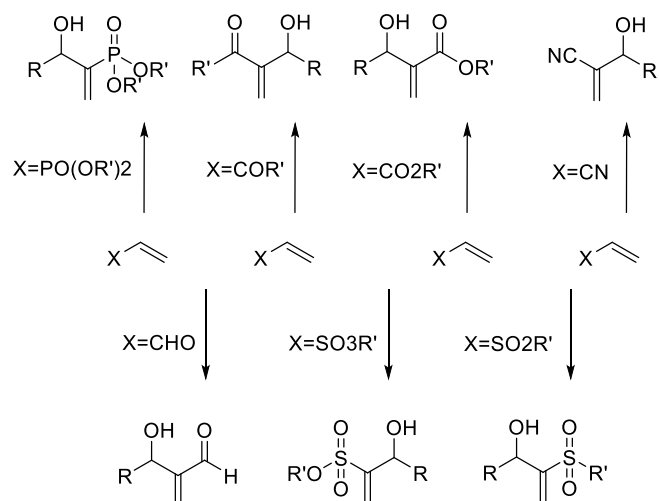


Figure 17. Versatility of the activated alkene within the Baylis-Hillman reaction.

Electrophile selection. Selection of the electrophile also allows for variability within the Baylis-Hillman reaction. The most common electrophiles include aldehydes, α -keto-esters, fluorinated ketones, and aldimines. All of these electrophile selections react at atmospheric pressure. An increase in pressure is required for ketones to react. In certain instances, without a good electrophile the alkene can dimerize (Figure 18)

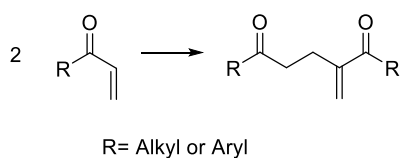


Figure 18. Dimerization of the alkene in the presence of a poor electrophile.

Choosing a catalyst. When it comes to the Baylis-Hillman reaction the catalyst is as equally as important as both the alkene and electrophile. The catalysts utilized in the Baylis-Hillman reaction are primarily unhindered and nucleophilic. An increase in the basicity of the catalyst tends to increase the rate of the reaction along with hydrogen bonding catalysts. Lanthanide Lewis acid triflates can also increase the rate of the reaction while stabilizing the zwitterion and/or activating the aldehyde present. The most common of Baylis-Hillman catalysts are DABCO, pyrrocoline, and quinuclidine (Figure 19).

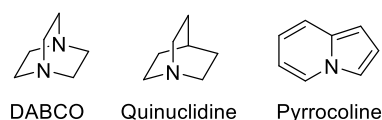


Figure 19. Common Baylis-Hillman catalysts.

Additional reaction conditions. Overall, the Baylis-Hillman reaction is relatively straightforward and simple reaction. A few additional factors can be taken into account to affect the reaction as a whole. In general, increasing the pressure increases the rate of the reaction. This can allow for an increase in the variety of substrates used while requiring less reactive catalysts such as triethylamine over DABCO. Hydrogen bonding via various solvents can also increase the rate of the Baylis-Hillman reaction. Uniquely, temperature effects are largely dependent upon the substrate being utilized. In certain instances

however, use of microwave can actually shorten the reaction time of the Baylis-Hillman reaction from days to mere minutes. Other options and advantages possible with the Baylis-Hillman reaction can include intramolecular reactions, E/Z selectivity, and asymmetric reactions to name a few.

Chapter 2

Synthesis of Polymers

Williamson Ether Synthesis

One of the initial reactions utilized in the synthesis of our polymers is based off of the Williamson ether synthesis named after Alexander William Williamson (Figure 20).

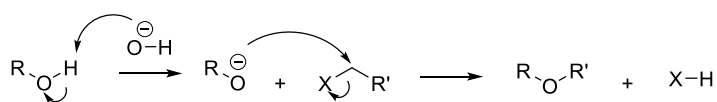


Figure 20. Reaction sequence of the Williamson ether synthesis.

The reaction involves utilizing a base to deprotonate an alcohol forming an alkoxide ion which reacts with an alkyl halide via an $\text{S}_{\text{N}}2$ reaction.

We began our synthesis with the coupling of 2-chloroethanol with phenols. Under the alkaline conditions, phenol could undergo alkylation directly with 2-chloroethanol or the latter could also undergo an intramolecular $\text{S}_{\text{N}}2$ reaction to furnish ethylene oxide (Figure 21). Ethylene oxide could eventually be attacked by the phenolate anion to produce 2-phenoxyethanol (Figure 22).

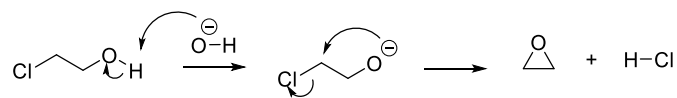


Figure 21. Mechanism of the formation of epoxide from 2-chloroethanol.

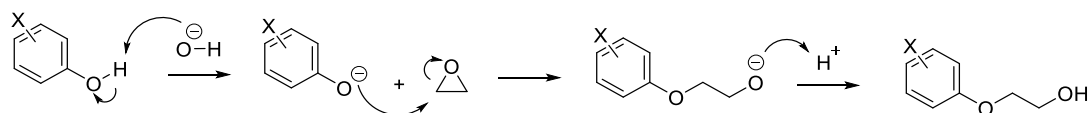


Figure 22. Secondary reaction of phenolic compounds reacting with formed epoxides.

Esterification

The next reaction in our syntheses involved converting the alcohol into an ester utilizing the nucleophilic addition of alcohol to acryloyl chloride (Figure 23).

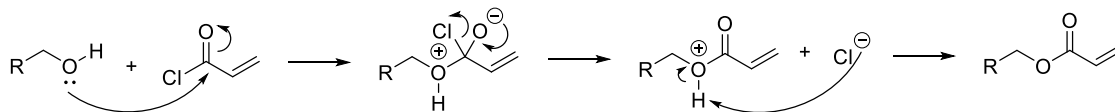


Figure 23. Esterification

Reduction of an Aldehyde to a Primary Alcohol

Another reaction utilized in our syntheses involved the reduction of aldehydes into primary alcohols using sodium borohydride (NaBH_4) (Figure 24).

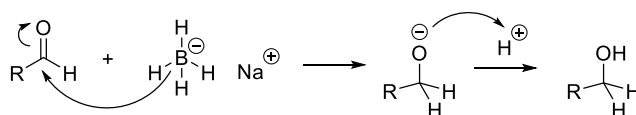


Figure 24. Reaction mechanism for the reduction of an aldehyde to a primary alcohol.

Conversion of Allylic Alcohols to Allyl Bromides

In one of our syntheses we focused on converting the allylic alcohol of the Baylis Hillman adduct into an allyl bromide utilizing hydrobromic acid and sulfuric acid. In the synthesis the sulfuric acid acts as a source of protons for protonation of the alcohol followed by the nucleophilic attack of the bromide ion to furnish the allylic bromide (Figure 25).

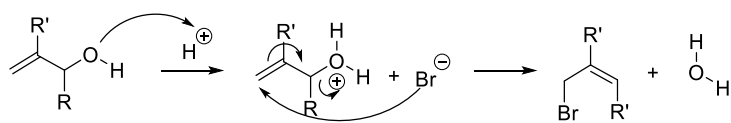


Figure 25. Conversion of an allylic alcohol to an allyl bromide.

Vanillin-Derived Methacrylate Polymers

Reaction scheme. The reaction scheme for the synthesis of vanillin-derived polymers began with commercially purchased vanillin as a substitute and comparative biomass-derived compound (Figure 26). The reaction of vanillin with chloroethanol under basic conditions proceeded as explained above and resulted in the formation of phenoxy alcohol **1**, which was then esterified with acryloyl chloride to yield the acrylate **2**. This acrylate was reacted with DABCO under Baylis-Hillman conditions which resulted in the formation of a polymer.

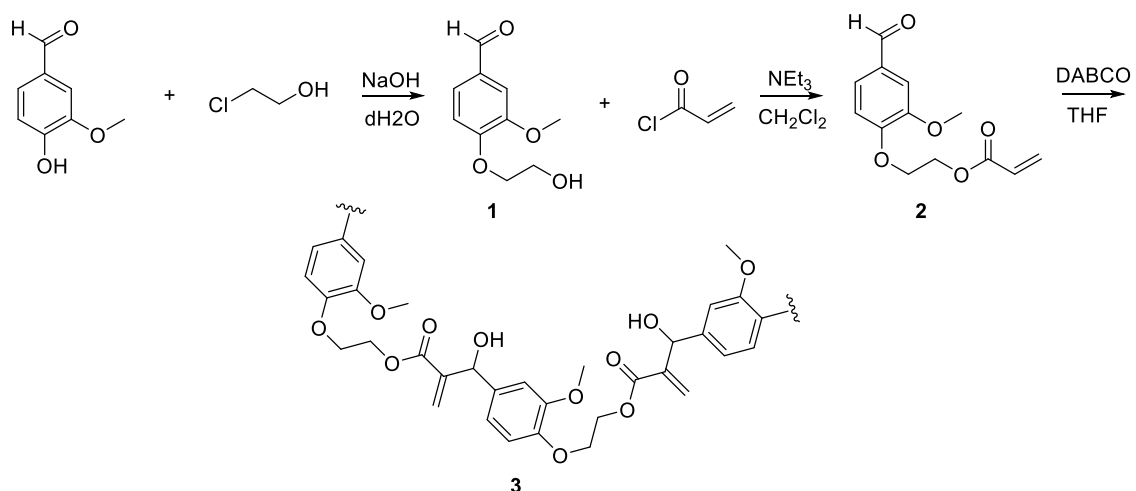


Figure 26. Vanillin-derived methacrylate polymers.

Synthesis of 4-(2-hydroxyethoxy)-3-methoxybenzaldehyde (1). A portion of vanillin (1.0 eq, 3.29 mmoles) was reacted under reflux for twenty hours with 2-chloroethanol (1.5 eq, 4.93 mmoles) in the presence of sodium hydroxide (1.5 eq, 4.93 mmoles) and water (10.0 mL) to yield a primary alcohol. Thin-layer chromatography confirmed completion of the reaction and the product was isolated through workup with 10% sodium hydroxide and dichloromethane. The organic product was dried over sodium sulfate and concentrated in vacuo utilizing a rotary evaporator. Average yield for step one of the reaction scheme was 60% crude off-white to pale brown product.

Synthesis of 2-(4-formyl-2-methoxyphenoxy)ethyl acrylate (2). Crude **1** (1.0 eq, 0.70 mmoles) was dissolved in dichloromethane (5.0 mL) and acryloyl chloride (1.5 eq, 1.05 mmoles) was slowly added at 0.0 °C. Triethylamine (3.0 eq, 2.09 mmoles) was added

dropwise at 0.0 °C, to the reaction vessel. The reaction was left to stir for sixteen hours while it was allowed to reach room temperature. Completion of the reaction was monitored via thin-layer chromatography. Upon completion, the reaction was worked up with dichloromethane and water. The product was dried over sodium sulfate and concentrated *in vacuo* resulting in yellow oil that recrystallized at room temperature with an average yield of 98% monomeric product.

Synthesis of vanillin-derived methacrylate polymers (3). **2** was recrystallized in methanol prior to polymer synthesis applications. The monomeric compound (1.0 eq, 0.65 mmol) underwent the Baylis-Hillman reaction by dissolving in tetrahydrofuran (1.0 mL) followed by the addition of the catalyst DABCO (0.2 eq, 0.13 mmol). The reaction completion was monitored via thin-layer chromatography and took approximately fourteen days to complete. Solvent levels were monitored periodically throughout the reaction sequence and maintained at the original volume level throughout the process by occasional addition of tetrahydrofuran. The product was purified to yield a white solid then analyzed utilizing gel permeation chromatography.

4-Hydroxybenzaldehyde-Derived Methacrylate Polymers

Reaction scheme. In a method similar to that of vanillin, p-hydroxybenzaldehyde was also employed for the formation of polymeric compound as shown in Figure 27.

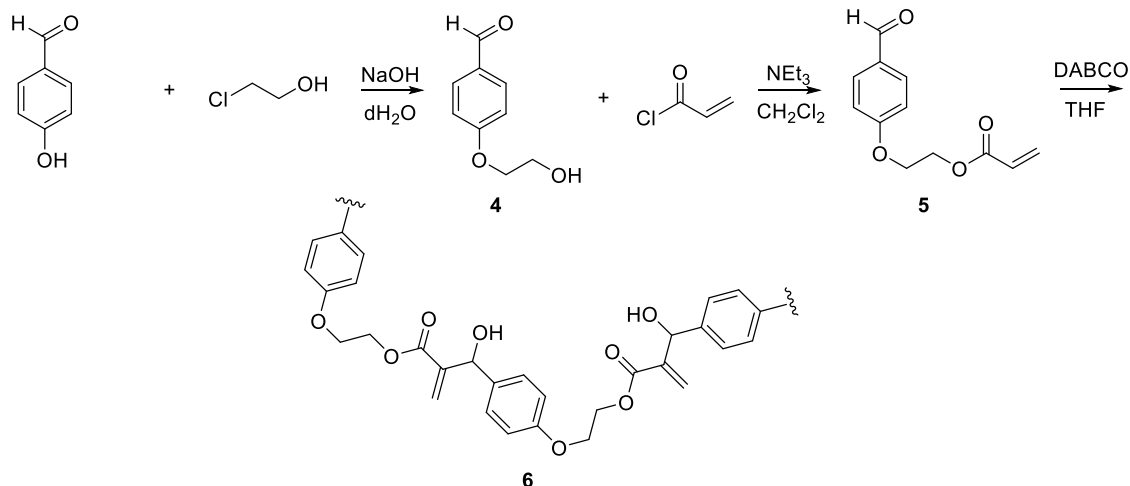


Figure 27. 4-Hydroxybenzaldehyde methacrylate polymers.

Synthesis of 4-(2-hydroxyethoxy)benzaldehyde (4). 4-hydroxybenzaldehyde (1.0 eq, 4.09 mmoles) was reacted utilizing the same conditions as that of the vanillin reaction. The reaction was conducted under reflux for twenty hours with 2-chloroethanol (1.5 eq, 6.14 mmoles) in the presence of sodium hydroxide (1.5 eq, 6.14 mmoles) and water (10.0 mL) to yield the primary alcohol. Thin-layer chromatography confirmed completion of the reaction and the product was isolated through workup with 10% sodium hydroxide and dichloromethane. The organic product was dried over sodium sulfate and concentrated *in vacuo* utilizing a rotary evaporator. The average yield for this product was 75% crude off-white product.

Synthesis of 2-(4-formylphenoxy)ethyl acrylate (5). Crude **4** (1.0 eq, 1.93 mmoles) was dissolved in dichloromethane (5.0 mL) and acryloyl chloride (1.5 eq, 2.88 mmoles)

was slowly added at 0.0 °C. Triethylamine (3.0 eq, 5.78 mmol) was added dropwise at 0.0 °C. The reaction was left to stir for sixteen hours while it was allowed to reach to room temperature. Completion of the reaction was monitored via thin-layer chromatography. Upon completion the reaction was worked up with dichloromethane and water. The product was dried over sodium sulfate and concentrated *in vacuo* resulting in yellow oil that also recrystallized at room temperature with an average yield of 98% monomeric product.

Synthesis of 4-hydroxybenzaldehyde-derived methacrylate polymers (6). Similar to **2, 5** was also recrystallized in methanol prior to polymer synthesis applications. The monomeric compound (1.0 eq, 1.19 mmol) underwent the Baylis-Hillman reaction by dissolving in tetrahydrofuran (1.0 mL) followed by the addition of the catalyst DABCO (0.2 eq, 0.24 mmol). The reaction completion was monitored via thin-layer chromatography and took approximately fourteen days to complete. Solvent levels were monitored periodically throughout the reaction sequence and maintained at the original volume level throughout the process by occasional addition of tetrahydrofuran. The product was purified to yield a white solid then analyzed for gel permeation chromatography.

Vanillin-Derived Bisacrylate Polymers

Reaction scheme. Vanillin was utilized as the starting material for this reaction sequence. Initially, vanillin was treated with 2-chloroethanol to produce phenoxyethanol which was subsequently reduced with NaBH₄ to yield hydroxymethylphenoxyethanol **7**. This was subsequently treated with 2 equivalents of acryloyl chloride to yield the

diacrylate. The diacrylate **8** was polymerized with terephthalaldehyde in the presence of DABCO under Baylis-Hillman conditions (Figure 28).

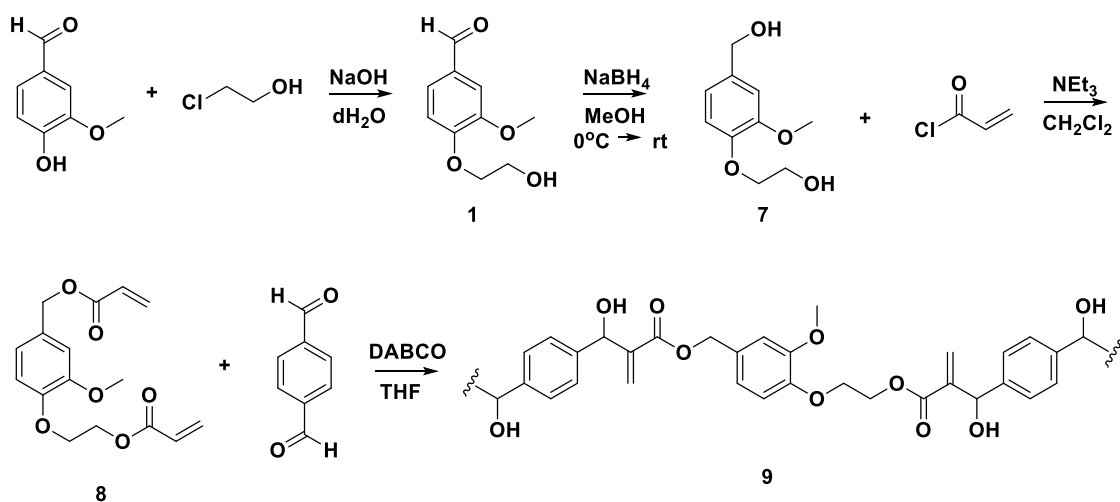


Figure 28. Vanillin-derived bisacrylate polymers.

Synthesis of 4-(2-hydroxyethoxy)-3-methoxybenzaldehyde (1). Vanillin (1.0 eq, 3.29 mmol) was reacted under reflux for twenty hours with 2-chloroethanol (1.5 eq, 4.93 mmol) in the presence of sodium hydroxide (1.5 eq, 4.93 mmol) and water to yield a primary alcohol. Thin-layer chromatography confirmed completion of the reaction and the product was isolated through workup with 10% sodium hydroxide and dichloromethane. The organic product was dried over sodium sulfate and concentrated in vacuo utilizing a

rotary evaporator. Average yield for step one of the reaction scheme was 60% crude off-white to pale brown product.

Synthesis of 2-(4-(hydroxymethyl)-2-methoxyphenoxy)ethan-1-ol (7). Crude **1** (1.0 eq, 8.87 mmol) was dissolved in methanol and sodium borohydride (4.0 eq, 35.47 mmol) was added slowly at room temperature. The reaction was left to stir for sixteen hours at room temperature. Completion of the reaction was monitored via thin-layer chromatography. Once complete, the reaction was concentrated *in vacuo*, mixed in water, and acidified to pH 7.0. The product was then isolated via workup with ethyl acetate, dried over sodium sulfate and concentrated *in vacuo* resulting in a white solid with an average yield of 62%.

Synthesis of ((acryloyloxy)ethoxy)-3-methoxybenzyl acrylate (8). **7** (1.0 eq, 0.61 mmol) was dissolved in dichloromethane. To this was added acryloyl chloride (2.2 eq, 1.33 mmol) at 0.0 °C followed by triethylamine (4.4 eq, 2.67 mmol) dropwise at 0.0 °C. The reaction was left to stir to room temperature for sixteen hours. Thin-layer chromatography verified the completion of the reaction and it was worked up with ethyl acetate, dried over sodium sulfate, and concentrated *in vacuo* resulting in a white solid with an average yield of 68%.

Synthesis of vanillin-derived bisacrylate polymers (9). Recrystallized **8** (1.0 eq, 0.43 mmol) underwent the Baylis-Hillman reaction by dissolving the recrystallized solid and terephthalaldehyde (1.0 eq, 0.43 mmol) in tetrahydrofuran followed by the addition of the catalyst DABCO (0.3 eq, 0.13 mmol). Thin-layer chromatography verified reaction completion after fourteen days. Solvent levels were monitored periodically throughout the

reaction and maintained throughout the process by occasional addition of tetrahydrofuran. The product was purified to yield a white solid and analyzed for gel permeation chromatography.

Terephthalaldehyde-Derived Bisacrylate Polymers

Reaction scheme. Following the use of terephthalaldehyde for the previous reaction we wanted to analyze a similar reaction sequence utilizing symmetrical aromatic diol **10**. This was synthesized by reducing terephthalaldehyde with sodium borohydride. The resulting product was then reacted with acryloyl chloride to yield a symmetrical bisacrylate followed by polymerization with additional terephthalaldehyde under Baylis-Hillman conditions (Figure 29).

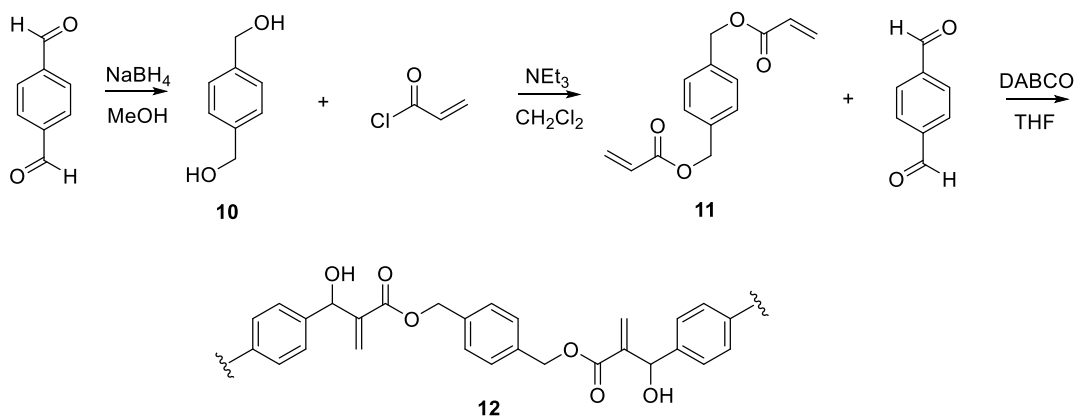


Figure 29. Synthesis of terephthalaldehyde-derived bisacrylate polymers.

Synthesis of 1,4-phenylenedimethanol (10). Commercially available terephthaldehyde (1.0 eq, 14.91 mmoles) was dissolved in methanol and sodium borohydride was then slowly added to this solution (4.0 eq, 59.64 mmoles), at 0.0 °C. Reaction was allowed to come to room temperature while stirring over a period of one hour. Completion of the reaction was monitored via thin-layer chromatography. The organic compound was extracted with ethyl acetate and dried over sodium sulfate. Concentration *in vacuo* yielded a white solid in 98% yield.

Synthesis of 1,4-phenylenebis(methylene) diacrylate (11). To **10** (1.0 eq, 3.62 mmoles) dissolved in dichloromethane was added acryloyl chloride (3.5 eq, 12.67 mmoles) at 0.0 °C. Triethylamine (7.0 eq, 25.33 mmoles) was added dropwise at 0.0 °C. The reaction was allowed to come to room temperature while stirring for sixteen hours. Thin-layer chromatography indicated the completion of reaction. Reaction was worked up with ethyl acetate, dried over sodium sulfate, and concentrated *in vacuo* to yield a pale red-orange oil that crystallized at room temperature. The average yield for the reaction was 70%.

Synthesis of terephthaldehyde-derived bisacrylate polymers (12). To **11** (1.0 eq, 0.37 mmoles) dissolved in tetrahydrofuran, was added terephthaldehyde (1.0 eq, 0.37 mmoles) and DABCO (0.3 eq, 0.11 mmoles). The reaction was left to stir for a period of fourteen days at which time Completion of the reaction was monitored via thin-layer chromatography.

Alternate Polymerization Reactions

Reaction scheme. We attempted the synthesis of polymeric materials using Baylis-Hillman reaction derived substrates to expand the scope of our work. Initial reaction of terephthalaldehyde with methyl acrylate yielded the bisallylic alcohol **13** which was then treated with HBr and H₂SO₄ to yield the bisallylic bromide **14**. Reaction of **14** with symmetric diamine (piperazine) then resulted in the formation of a polymer **15** (Figure 30).

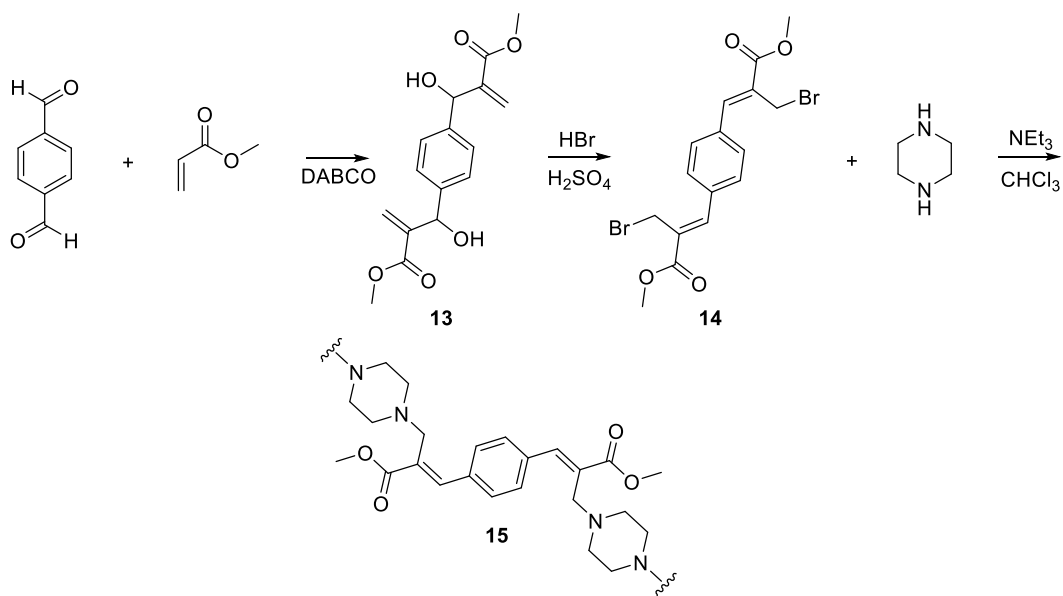


Figure 30. Reaction scheme of terephthalaldehyde/methacrylate & piperazine polymers.

Dimethyl 2,2'-(1,4-phenylenebis(hydroxymethylene))diacrylate (13).

Terephthaldehyde (1.0 eq, 37.28 mmoles) was reacted with methyl acrylate (9.0 eq, 335.50 mmoles) and DABCO (0.6 eq, 22.37 mmoles) in a suitable reaction vessel for a period of fourteen days. Thin-layer chromatography showed that the reaction was complete and the system was worked up with ethyl acetate. The compound was then washed with brine and dried over sodium sulfate prior to concentrating *in vacuo* to yield approximately 96% crude product.

Dimethyl 3,3'-(1,4-phenylene)(2Z,2'Z)-bis(2-(bromomethyl)acrylate) (14). Crude **13** (1.0 eq, 0.82 mmoles) was reacted with hydrobromic acid (45.0 eq, 36.74) at room temperature. To the system was added sulfuric acid (3.4 eq, 2.78 mmoles) and the reaction was left to stir for three hours. Thin-layer chromatography verified the completion of the reaction. The compound was extracted with chloroform and washed with brine. It was then dried over sodium sulfate and concentrated *in vacuo* with an average yield of approximately 75%

Terephthaldehyde-derived methacrylate & piperazine based polymers (15).

Piperazine (2.0 eq, 1.16 mmoles) and triethylamine (24.0 eq, 13.89 mmoles) were stirred in chloroform for fifteen minutes to affect dissolution. To the reaction mixture was then added a solution of **14** (1.0 eq, 0.58 mmoles) dissolved in 3 mL chloroform. The reaction was complete after three hours as verified by thin-layer chromatography. The mixture was concentrated *in vacuo* and worked up with 5% aqueous hydrochloric acid, chloroform, and washed with brine. The pH of the aqueous layer was neutralized to pH 7.0 to yield a white-

yellow solid precipitate. The solid was filtered and dried *in vacuo* resulting in a relatively pure compound.

In addition to the previously mentioned product, an additional polymer was also synthesized with the starting material terephthalaldehyde. For this reaction sequence terephthalaldehyde was reduced with sodium borohydride to yield the diol, which was then reacted with hydrobromic acid to yield a di-bromide. The dibromide compound was then reacted with piperazine to yield a polymer of alternating piperazine and aromatic groups (Figure 31).

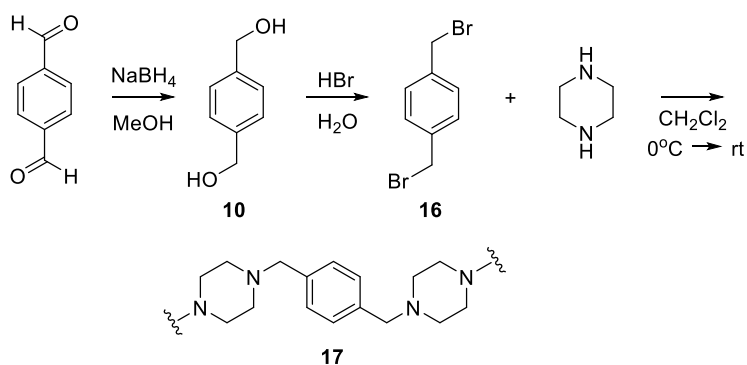


Figure 31. Reaction scheme of terephthalaldehyde & piperazine based polymers.

Synthesis of 1,4-phenylenedimethanol (10). The synthesis follows the same preparation as previously mentioned. Terephthalaldehyde (1.0 eq, 14.91 mmoles) was dissolved in methanol and reduced to the diol by slow addition of Sodium Borohydride

(4.0 eq, 59.64 mmols) at 0.0 °C. The reaction was allowed to come to room temperature while stirring over a period of one hour. Completion of the reaction was monitored via thin-layer chromatography and extraction was completed by ethyl acetate. The compound was then dried over sodium sulfate and concentrated *in vacuo* to yield a white solid in 98% yield.

Synthesis of 1,4-bis(bromomethyl)benzene (16). **10** (1.0 eq, 7.24 mmols) was added to a 48% hydrobromic acid solution (16.0 eq, 115.80 mmols) and allowed to stir at room temperature for two hours. The resulting red-orange solid was then consequently recrystallized in methanol to afford a pale orange/white solid in 96% yield.

Synthesis of terephthaldehyde & piperazine based polymers (17). The synthesis of the polymer began by dissolving anhydrous piperazine (2.0 eq, 0.76 mmols) in chloroform followed by the drop-wise addition of a solution of **16** (1.0 eq, 0.38 mmols) in 5 mL chloroform at 0.0 °C. The completion of the reaction was monitored via thin-layer chromatography and took approximately six hours at room temperature. The reaction was worked up with chloroform and the organic layer dried over sodium sulfate and concentrated *in vacuo*. The crude product was then recrystallized in hexane to yield the final product.

Characterization data for all of these compounds and polymers are shown in Chapter 3.

Chapter 3

Data

Identification & Characterization

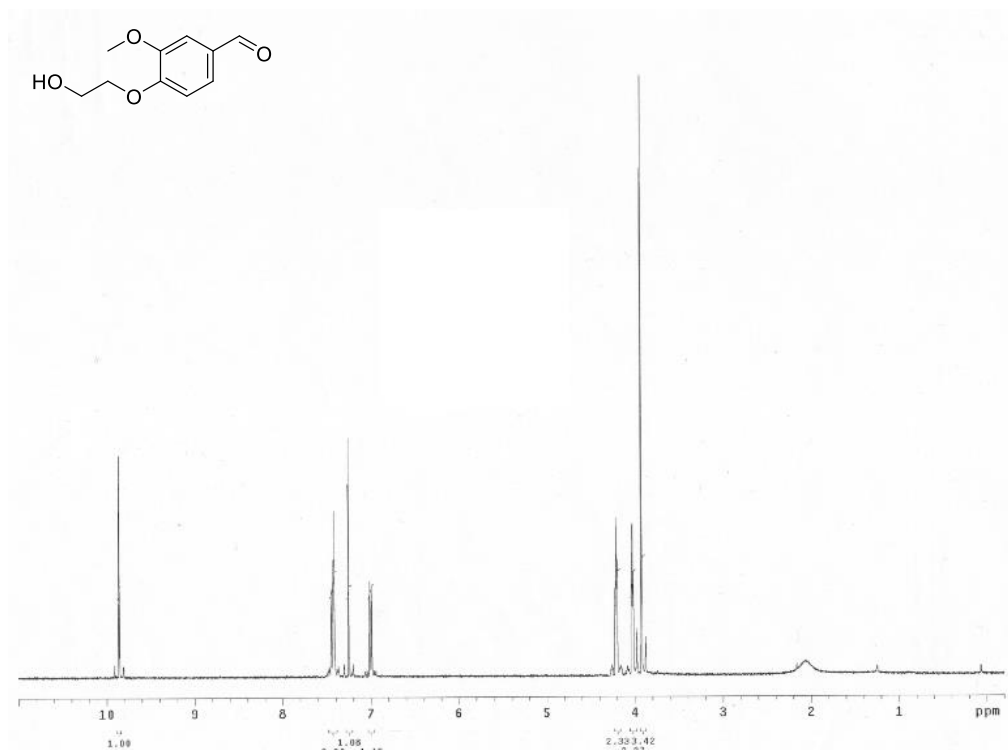


Figure 32. 400 MHz ¹H NMR of Compound 1 in CDCl₃

δ 9.85 (s, 1H), 7.43 (d, $J = 12.0$ Hz, 1H), 7.25 (s, 1H), 7.00 (d, $J = 6.0$ Hz 1H), 4.21 (t, $J = 4.6$ Hz 2H), 4.03 (t, $J = 3.8$ Hz 2H), 3.93 (s, 3H)

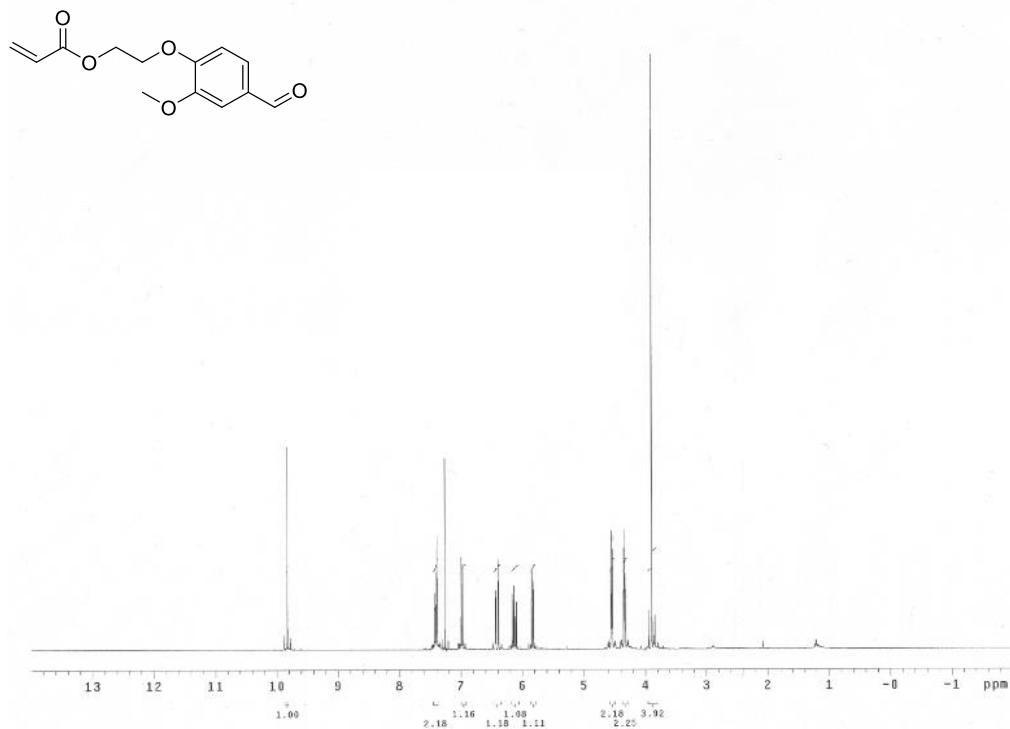
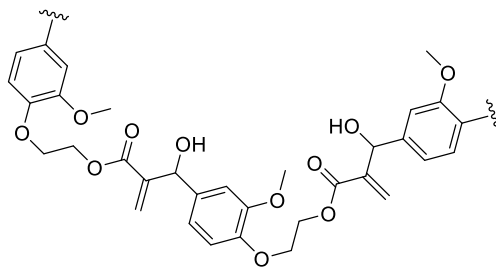


Figure 33. 400 MHz ¹H NMR of Compound 2 in CDCl₃

δ 9.85 (s, 1H), 7.81 (d, $J = 8.4$ Hz, 1H), 7.25 (s, 1H), 7.00 (d, $J = 7.2$ Hz, 1H), 6.42 (d, $J = 17.2$ Hz, 1H), 6.13 (t, $J = 10.4$ Hz, 1H), 5.84 (d, $J = 10.4$ Hz, 1H), 4.51 (t, $J = 4.4$ Hz, 2H), 4.27 (t, $J = 4.0$ Hz, 2H), 3.93 (s, 3H)



Gel Permeation Chromatography Analysis

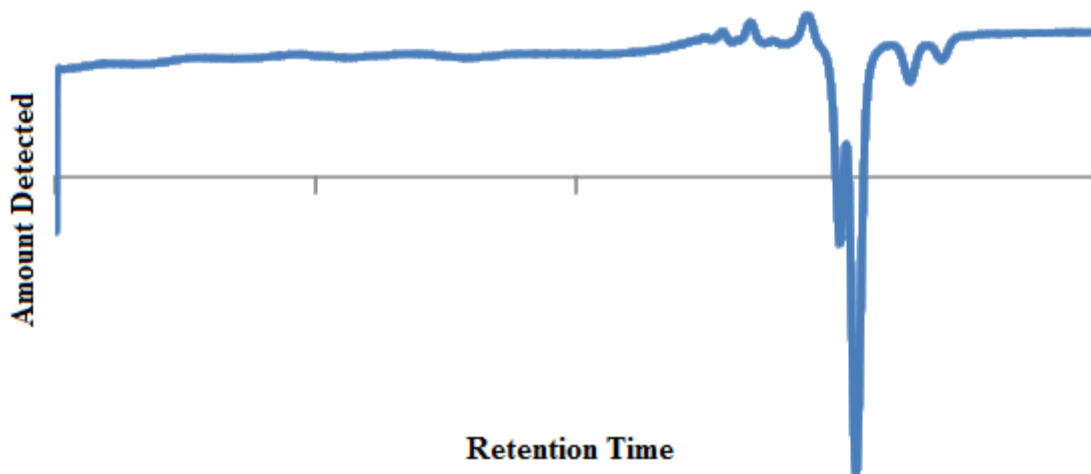


Figure 34. GPC Spectrum of Compound 3

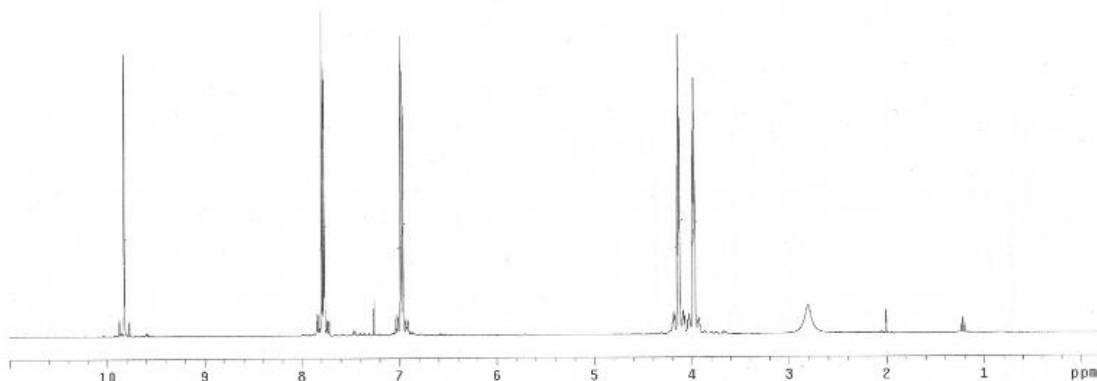
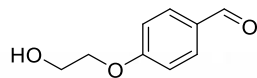


Figure 35. 400 MHz ^1H NMR of Compound **4** in CDCl_3

δ 9.85 (s, 1H), 7.82 (d, $J = 6.0$ Hz, 2H), 7.00 (d, $J = 6.4$ Hz, 2H), 4.16 (t, 4.0 Hz, 2H), 4.01 (t, 3.6 Hz, 2H)

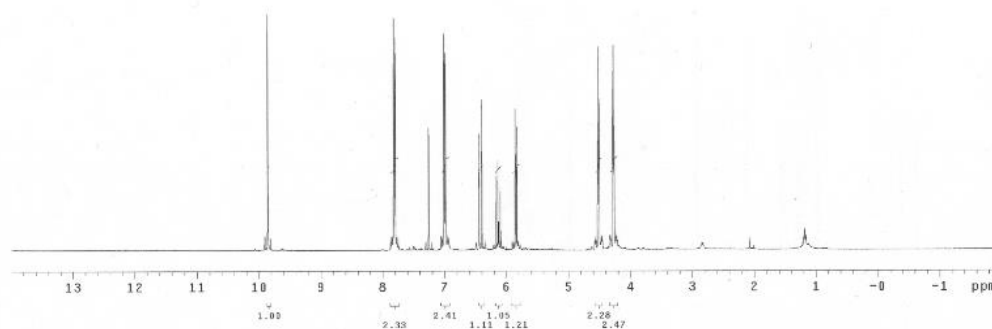
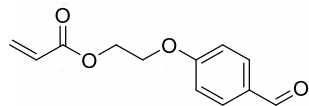


Figure 36. 400 MHz ^1H NMR of Compound **5** in CDCl_3

δ 9.87 (s, 1H), 7.82 (d, $J = 6.4$ Hz, 2H), 7.01 (d, $J = 6.8$ Hz, 2H), 6.43 (d, $J = 17.2$ Hz, 1H), 6.14, (t, $J = 7.6$ Hz, 1H), 5.85 (d, $J = 9.6$ Hz, 1H), 4.53 (t, 4.0, 2H), 4.29 (t, $J = 3.6$ Hz, 2H)

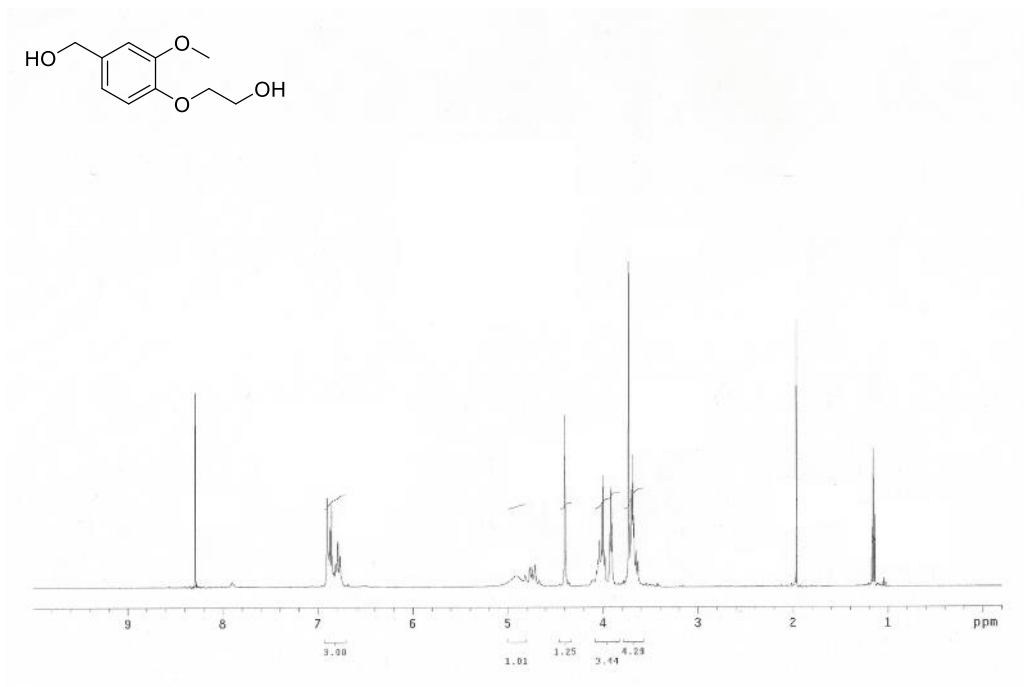


Figure 38. 400 MHz ¹H NMR of Compound 7 in DMSO – d₆

δ 6.90 (s, 1H), 6.86 (d, $J = 7.6$ Hz, 1H), 6.77 (d, $J = 8.0$ Hz, 1H), 4.40 (s, 2H), 4.00 (t, $J = 7.0$ Hz, 2H), 3.92 (t, $J = 4.8$ Hz, 2H), 3.72 (s, 3H)

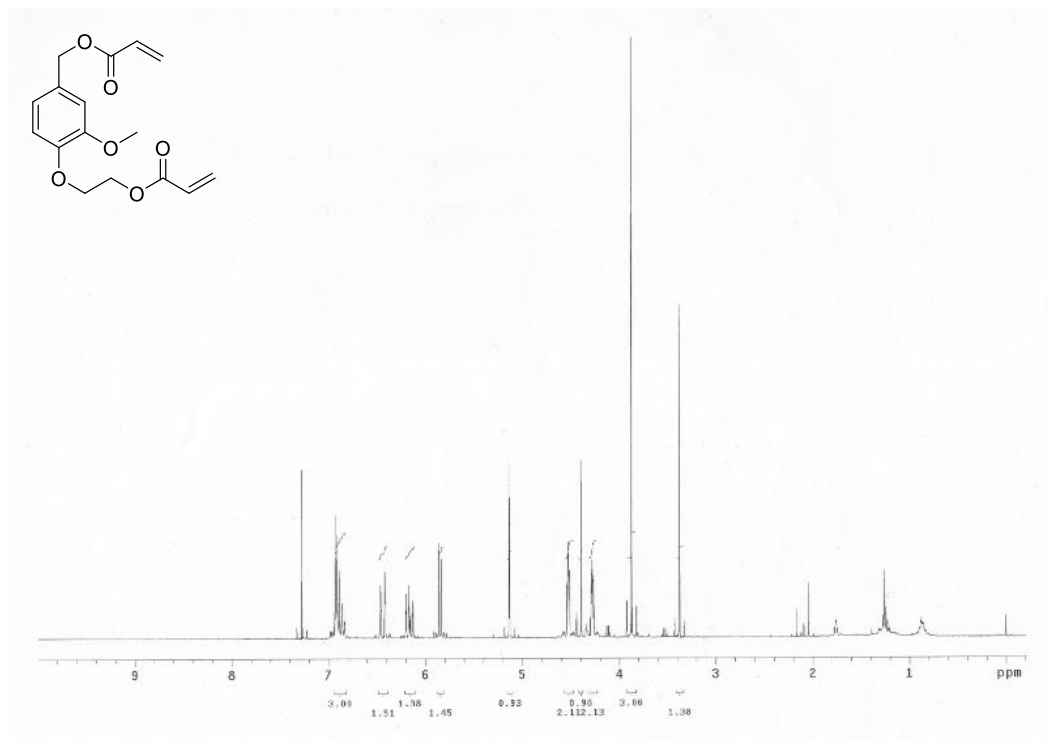


Figure 39. 400 MHz ^1H NMR of Compound **8** in DMSO – d_6

δ 6.89 (m, $J = 6.0$ Hz, 3H), 6.43 (d, $J = 15.2$ Hz, 2H), 6.16 (t, $J = 10.8$ Hz, 2H), 5.86 (d, $J = 10.0$ Hz, 2H), 5.14 (s, 2H), 4.53 (t, $J = 4.8$ Hz, 2H), 4.28 (t, $J = 2.8$ Hz, 2H) 3.87 (s, 3H)

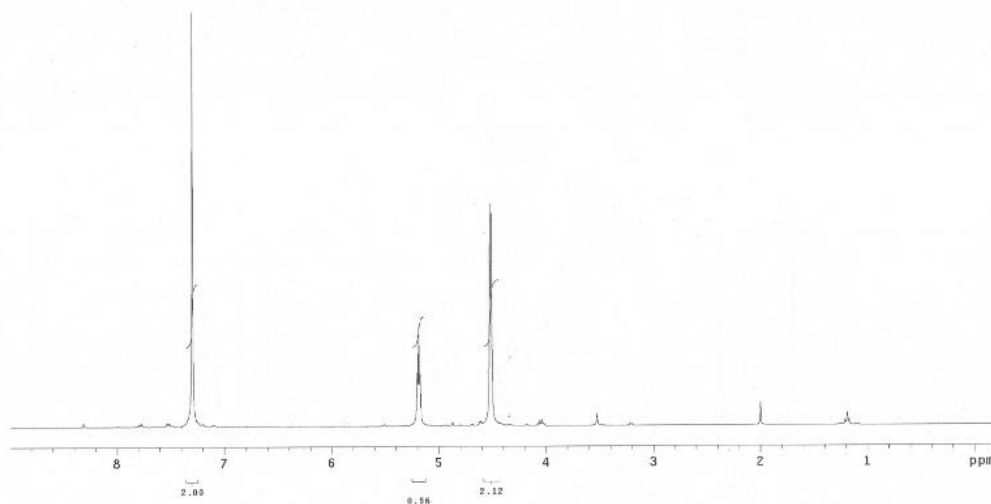
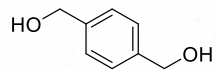


Figure 41. 400 MHz ^1H NMR of Compound **10** in CDCl_3

δ 7.25 (s, 4H), 5.20 (s, 2H), 4.45 (s, 4H)

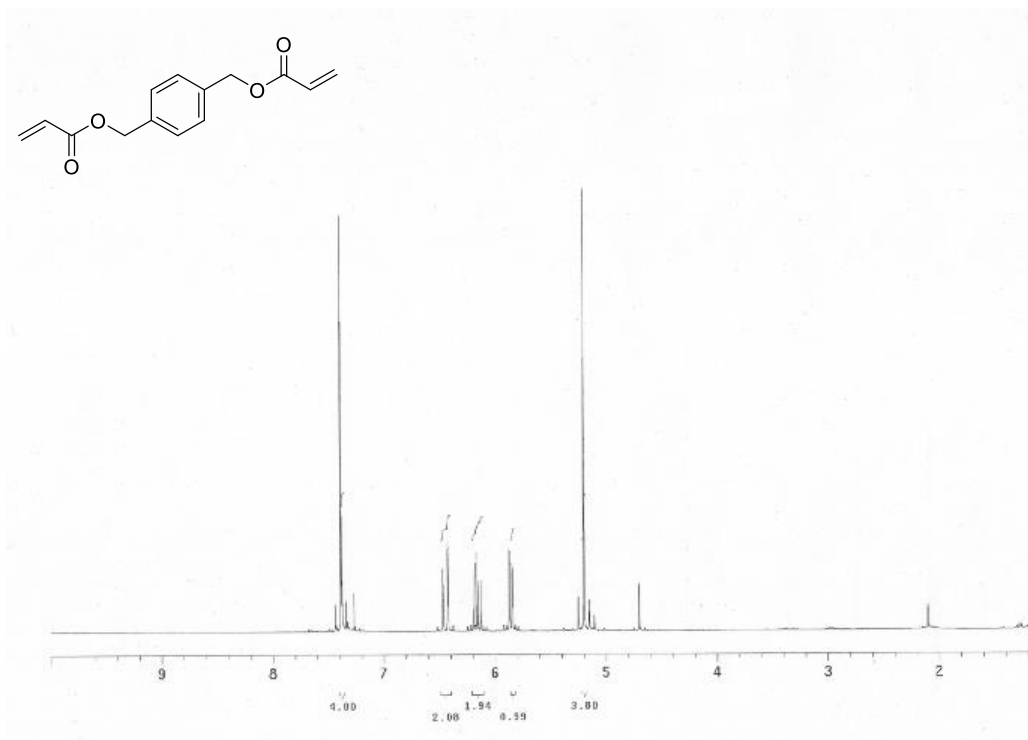


Figure 42. 400 MHz ¹H NMR of Compound **11** in CDCl₃

δ 7.39 (s, 4H), 6.45 (d, $J = 16.0$ Hz, 2H), 6.16 (t, $J = 6.8$ Hz, 2H), 5.86 (d, $J = 10.0$ Hz, 2H), 5.21 (s, 4H)

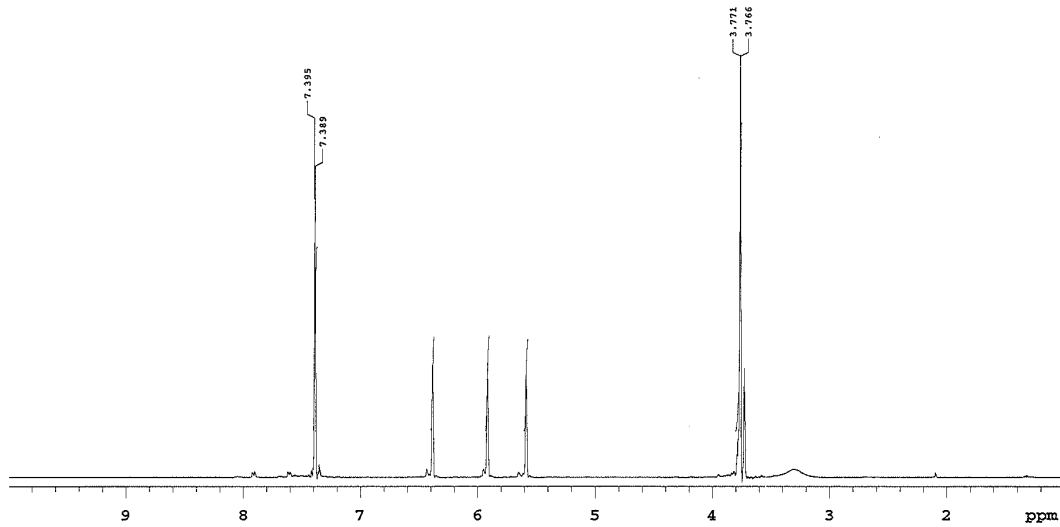
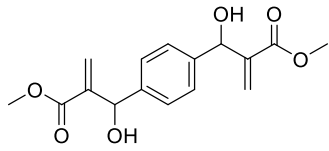


Figure 43. 400 MHz ^1H NMR of Compound **12** in CDCl_3

δ 7.39 (s, 4H), 6.38 (s, 2H), 5.92 (s, 2H), 5.60 (s, 2H), 3.77 (s, 6H)

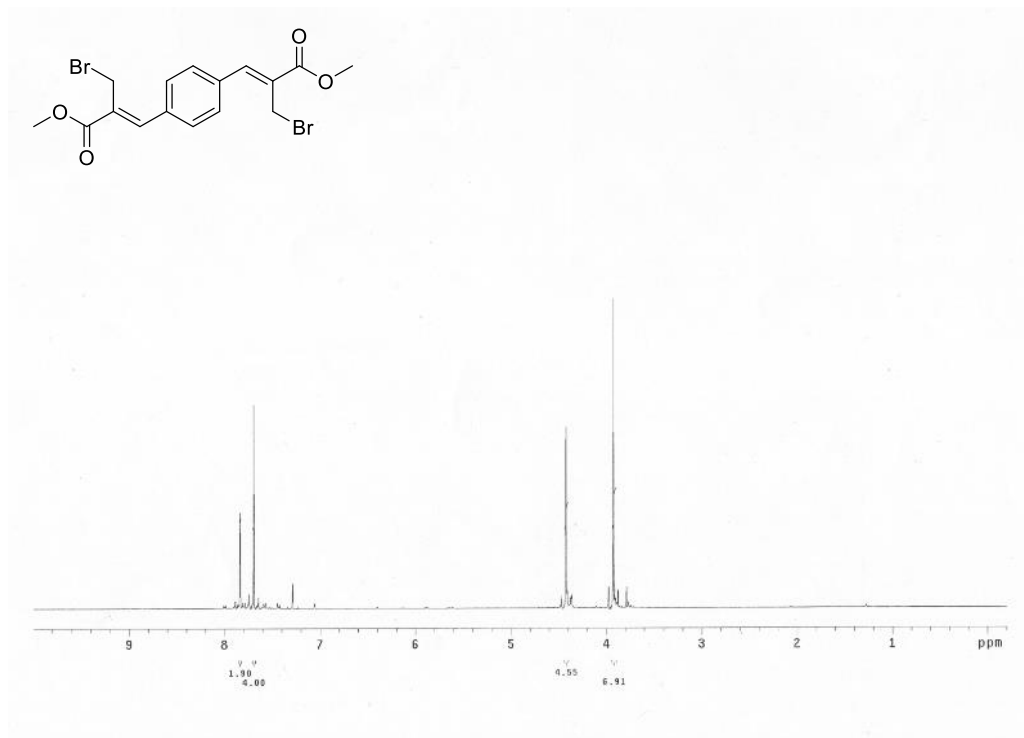


Figure 44. 400 MHz ¹H NMR of Compound **13** in CDCl₃

δ 7.83 (s, 2H), 7.65 (s, 4H), 4.42 (s, 4H), 3.93 (s, 6H)

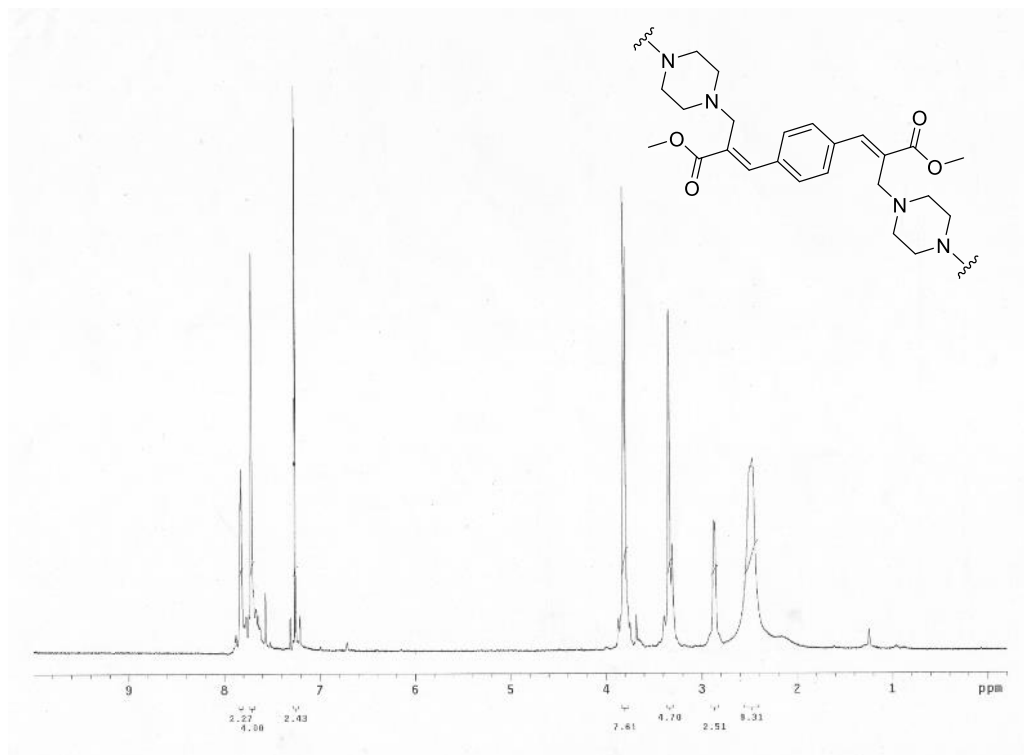


Figure 45. 400 MHz ¹H NMR of Compound **14** in CDCl₃

δ 7.83 (s, 2H), 7.71 (s, 4H), 3.82 (s, 8H), 3.36 (s, 6H), 2.91 (s, 3H)

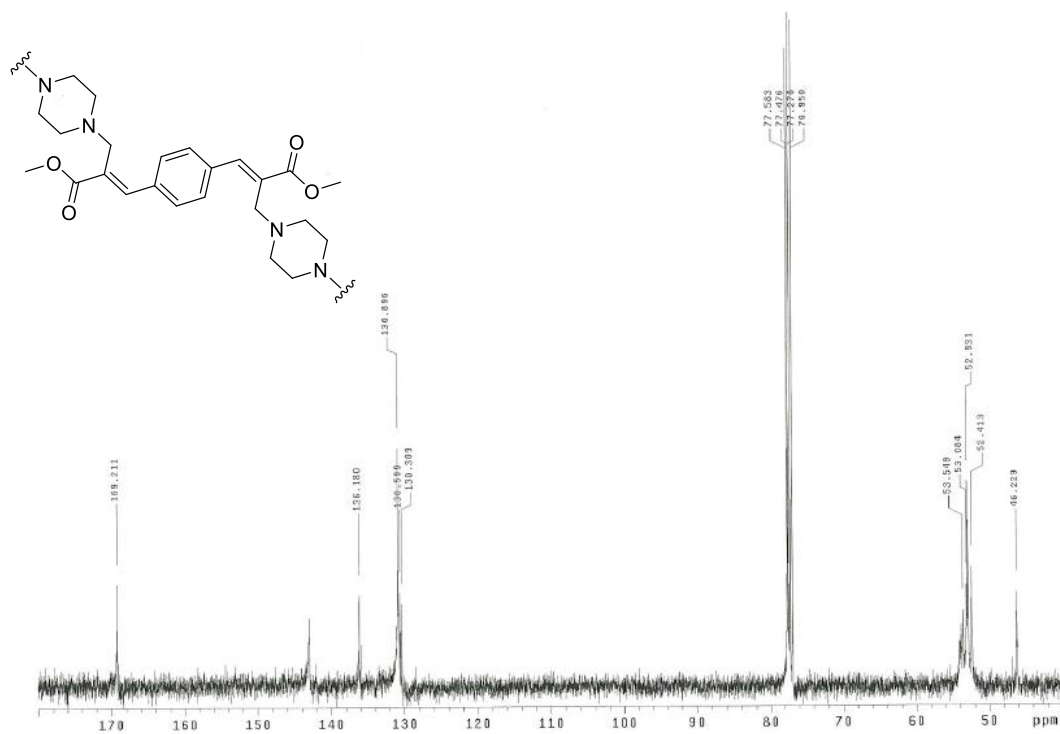


Figure 46. 101 MHz ^{13}C NMR of Compound **14** in CDCl_3

δ 169.2, 143.6, 136.4, 130.6, 130.5, 130.5, 53.2, 53.3

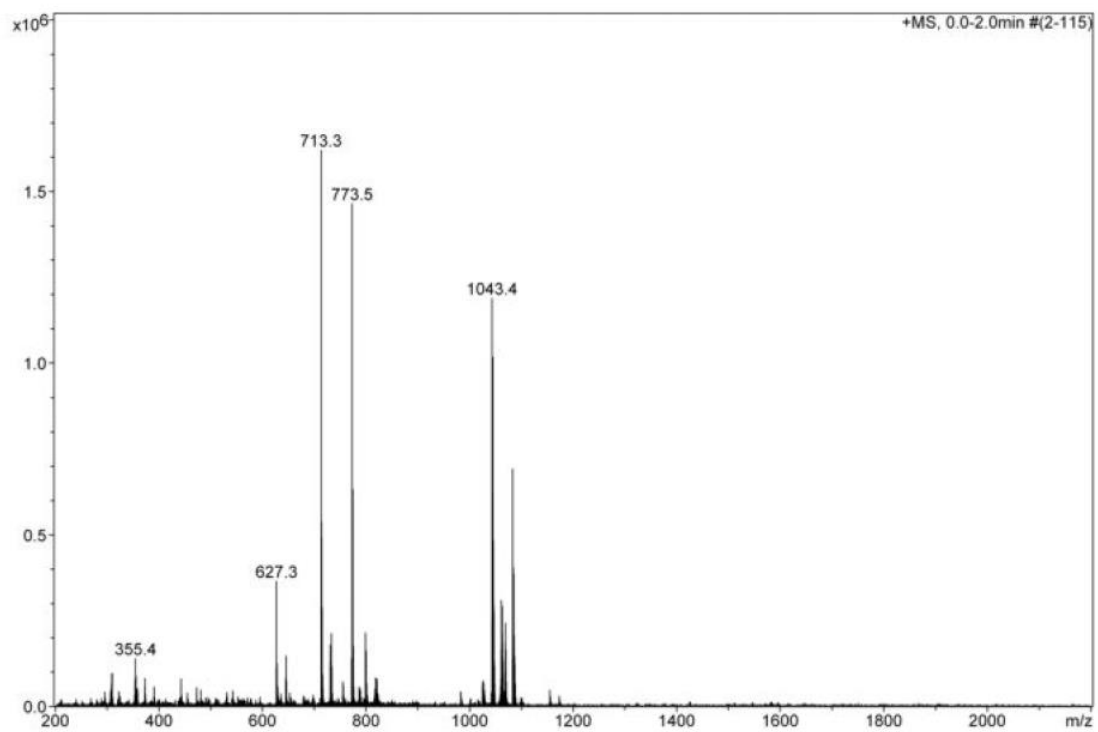
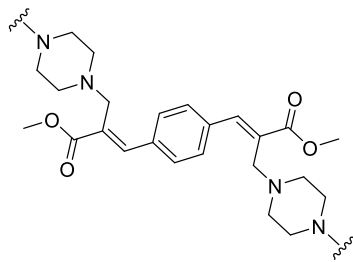


Figure 47. MS Analysis for Compound 14.

ESI – MS: m/z 1080

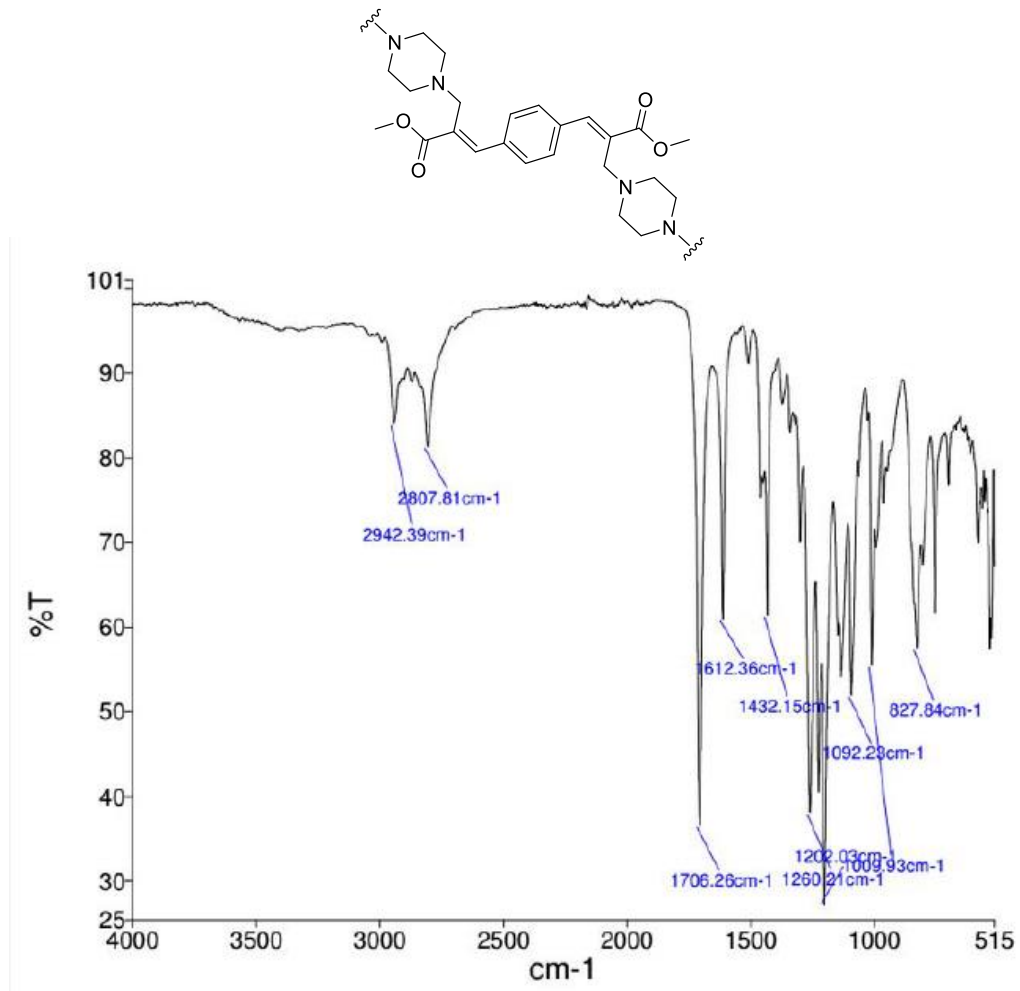


Figure 48. IR Spectrum of Compound 14.

IR (neat): 2942, 2808, 1706, 1612, 1432, 1260, 1202, 1092, 1010, 828 cm^{-1} .

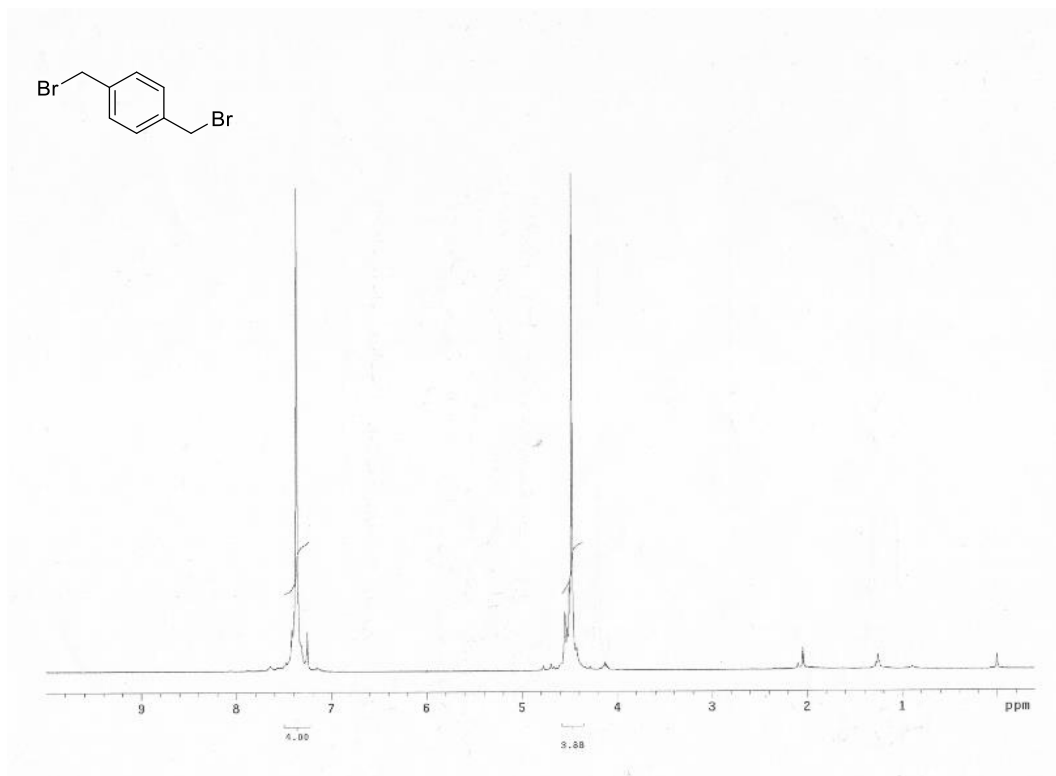


Figure 49. 400 MHz ^1H NMR of Compound **16** in CDCl_3

δ 7.19 (s, 4H), 4.49 (s, 4H).

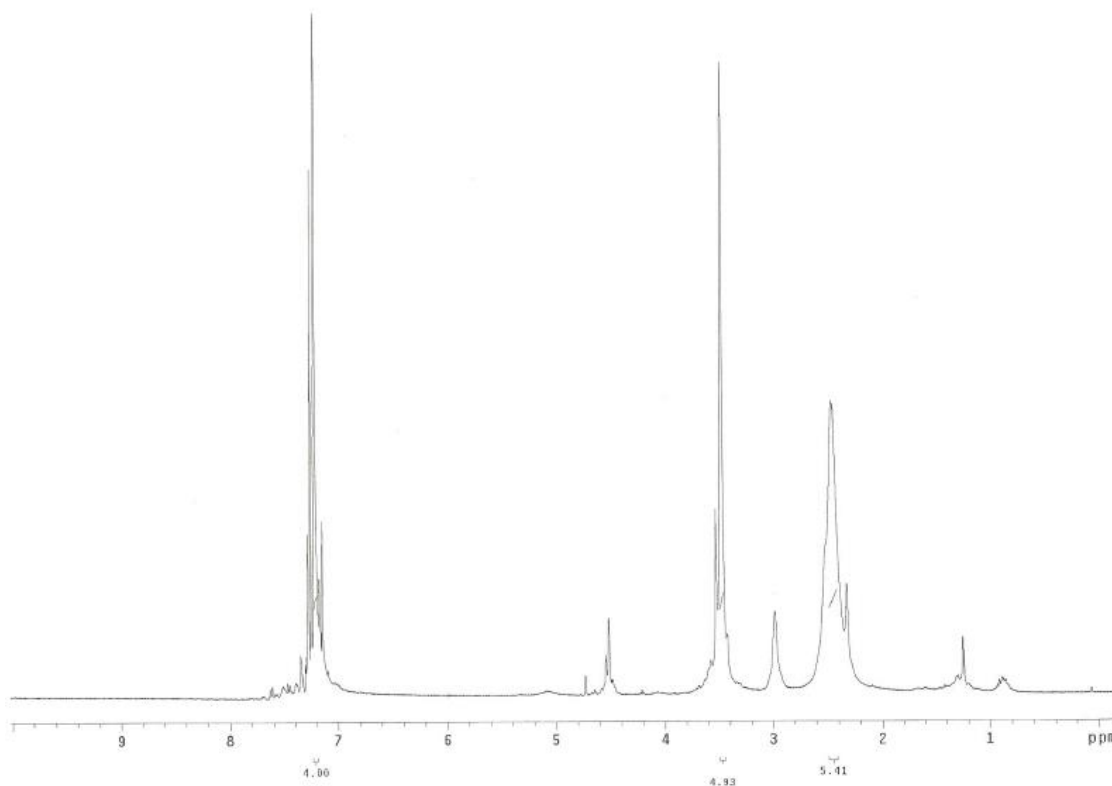
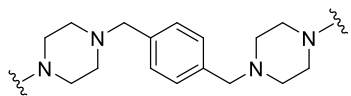


Figure 50. 400 MHz ^1H NMR of Compound **17** in CDCl_3

δ 7.21 (s, 4H), 3.51 (s, 4H), 2.43 (s, 4H)

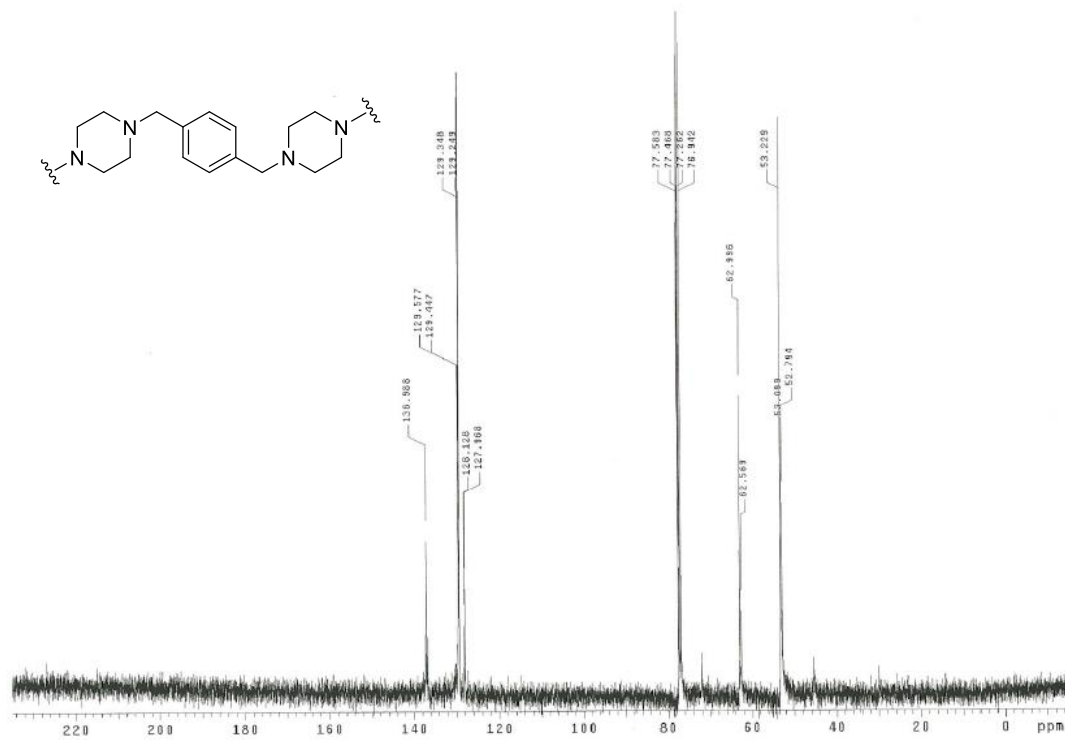


Figure 51. 101 MHz ¹³C NMR of Compound **17** in CDCl₃

δ 137.0, 129.6, 63.0, 53.2.

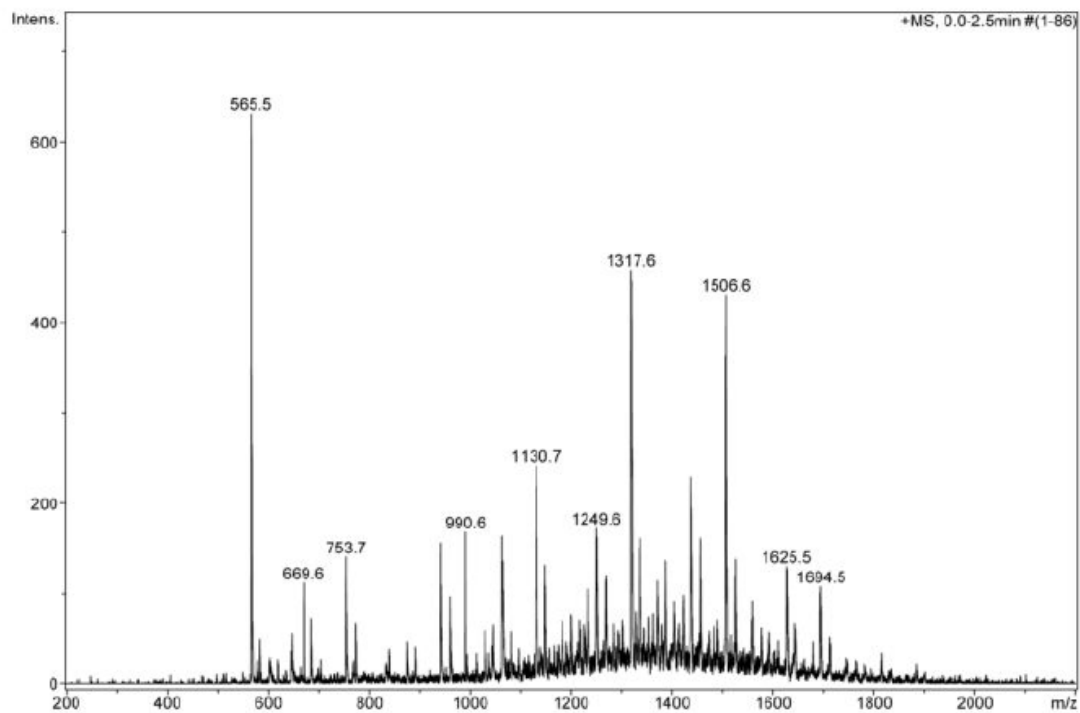
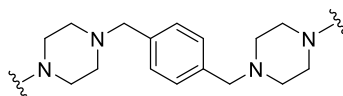


Figure 52. MS Analysis for Compound 17.

ESI – MS: m/z 1695

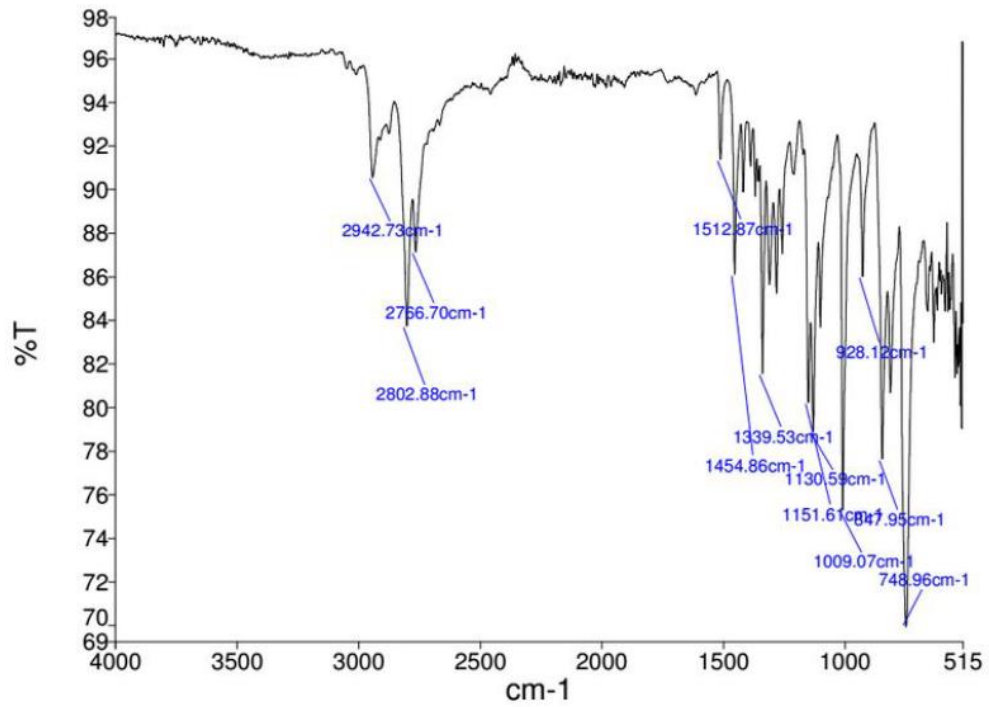
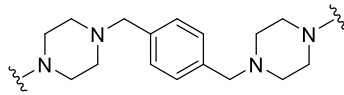


Figure 53. IR Spectrum of Compound 17.

IR (neat): 2943, 2803, 2767, 1513, 1455, 1340, 1152, 1131, 1009, 928, 848, 749.

References

1. Siman, P.; Filipova, A.; Alena, Tichá, A.; Niang, M.; Bezrouk, A.; Havelek, R. Effective method of purification of betulin from birch bark: The importance of its purity for scientific and medicinal use. *PLoS One*. **2016**. *11*, 1-16.
2. Yang, S. J.; Liu, M. C.; Xiang, H. M.; Zhao, Q.; Xue, W.; Yang, S. Synthesis and in vitro antitumor evaluation of betulin acid ester derivatives as novel apoptosis inducers. *Eur. J. Med. Chem.* **2015**. *102*, 249-255.
3. Park, J. H.; Ye, M.; & Park, K. Biodegradable polymers for microencapsulation of drugs. *Molecules*. **2005**. *10*, 146-161.
4. Shahani, S. Global markets and technologies for advanced drug delivery systems. *BCC Research*. **2014**.
5. Grund, S.; Bauer, M.; Fischer, D. Polymers in drug delivery-state of the art and future trends. *Adv. Eng. Mater.* **2011**. *13*, B61-B87.
6. Tiwari, G.; Tiwari, R.; Sriwastawa, B.; Bhati, L.; Pandey, S.; Pandey, P.; Bannerjee, S. Drug delivery systems: an updated review. *Int. J. Pharm. Investig.* **2012**. *2*, 2-11.
7. Angelova, N.; Hunkeler, D. Rationalizing the design of polymeric biomaterials. *Trends in Biotechnol.* **1999**. *10*, 409-421.
8. Pillai, O.; Panchagnula, R. Polymers in drug delivery. *Curr. Opin. Chem. Biol.* **2001**. *5*, 447-451.
9. Elbert, D. L.; Hubbell, J. A. Surface treatments of polymers for biocompatibility. *Annual Review of Materials Research*. **1996**. *26*, 365.
10. Archana, J.; Shore, A. M.; Jonnalagadda, S. C.; Ramanujachary, K. V.; Mugweru, A. Conversion of fructose, glucose and sucrose to 5-hydroxymethyl-2-furfural over mesoporous zirconium phosphate catalyst. *Appl. Catal., A* **2015**. *489*, 72-76.
11. Jain, A. J.; Jonnalagadda, S. C.; Ramanujachary, K. V.; Mugweru, A. Selective oxidation of 5-hydroxymethyl-2-furfural to furan-2,5-dicarboxylic acid over spinel mixed metal oxide catalyst. *Catal. Commun.* **2015**. *58*, 179-182.
12. Domling, A.; Ugi, I. Multicomponent reactions with isocyanides. *Angew. Chem. Int. Ed.* **2000**. *30*, 3168-3210.
13. Ugi, I.; Fetzer, U.; Eholzer, U.; Knupfer, U.; Offermann, K. Isonitrile syntheses. *Angew. Chem. Int. Ed.* **1965**. *4*, 474-484.

14. Passerini, M.; Simone, L. *Gazz. Chim. Ital.* **1921**. *51*, 126-129.
15. Banfi, L.; Riva, R. The passerini reaction. *Org. React.* **2005**. *65*, 1-140.
16. Kreye, O.; Tóth, T.; Meier, M. A. R. Introducing multicomponent reactions to polymer science: Passerini reactions of renewable monomers. *J. Am. Chem. Soc.* **2011**. *133*, 1790-1792.
17. Denmark, S. E.; Fan, Y. Catalytic, enantioselective α -additions of isocyanides: Lewis base catalyzed Passerini-type reactions. *J. Org. Chem.* **2005**. *70*, 9667-9676.
18. Basavaiah, D.; Rao, P. D.; Hyma, R. S. The Baylis-Hillman reaction: A novel carbon-carbon bond forming reaction. *Tetrahedron.* **1996**. *52*, 8001-8062.
19. Price, K. E.; Broadwater, S. J.; Jung, H. M.; McQuade, D. T. Baylis-Hillman mechanism: A new interpretation in aprotic solvents. *Org. Lett.* **2004**. *7*, 147-150.
20. Price, K.E.; Broadwater, S. J.; Walker, B., J.; McQuade, D. T. A new interpretation of the Baylis-Hillman mechanism. *J. Org. Chem.* **2005**. *70*, 3980-3987.
21. Robiette, R.; Aggarwal, V. K.; Harvey, J. N. Mechanism of the Morita-Baylis-Hillman reaction: A computational investigation. *J. Am. Chem. Soc.* **2007**. *129*, 15513-15525.
22. Agrawal, P. Significance of polymers in drug delivery system. *J. Pharmacovigil.* **2014**. *3*.
23. Bridgwater, A.V.; Peacocke, G. V. C. Fast pyrolysis processes for biomass. *Renew. Sustainable Energy Rev.* **2000**. *4*, 1-73.
24. Briens, C.; Piskorz, J.; Franco, B. Biomass valorization for fuel and chemicals production -- a review. *Int. J. Chem. Reactor Eng.* **2008**. *6*.
25. Christensen, C. H.; Rass-Hansen, J.; Marsden, C. C.; Taarning, E.; Egeblad, K. The renewable chemicals industry. *ChemSusChem.* **2008**. *1*, 283-289.
26. Gallezot, P. Catalytic conversion of biomass: challenges and issues. *ChemSusChem.* **2008**. *1*, 734-737.
27. Hejazi, R.; Amiji, M. Chitosan-based gastrointestinal delivery systems. *J. Controlled Release.* **2003**. *89*, 151-165.
28. Hill, J. S.; Isaacs, N. S. Mechanism of α -substitution reactions of acrylic derivatives. *J. Phys. Org. Chem.* **1990**. *3*, 285-288.

29. Jeong, B.; Bae, Y. H.; Lee, D. S.; Kim, S. W Biodegradable block copolymers as injectable drug delivery systems. *Nature*. **1997**. 388, 860-862.
30. Liechty, W. B.; Kryscio, D. R.; Slaughter, B. V.; Peppas, N. A. Polymers for drug delivery systems. *Annu. Rev. Chem. Biomol. Eng.* **2010**. 1, 149-173.
31. Nel, W. P.; Cooper, C. J. Implications of fossil fuel constraints on economic growth and global warming. *Energy Policy*. **2009**. 37, 166–180.
32. Passerini, M.; Ragni, G. *Gazz. Chim. Ital.*. **1931**. 61, 964-969.
33. Pekarek, K.J.; Jacob, J.S.; Mathiowitz, E. Double-walled polymer microspheres for controlled drug release. *Nature*. **1994**. 367, 258-260.
34. Román-Leshkov, Y.; Chheda, J. N.; Dumesic, J. A. Phase modifiers promote efficient production of hydroxymethylfurfural from fructose. *Science*. **2006**. 312, 1933–1937.
35. Rubio Rodriguez, M. A.; Ruyck, J. D.; Diaz, P. R.; Verma, V. K.; Brann, S. An LCA based indicator for evaluation of alternative energy routes. *Appl. Energy*. **2011**. 88, 630-635.
36. Ulbrich, K.; Pechar, M.; Strohm, J.; Subr, V.; Rihova, B. Synthesis of biodegradable polymers for controlled drug release. *Ann. N. Y. Acad. Sci.* **1997**. 831, 47-56.
37. Vogelson, C. T. Advances in drug delivery systems. *Mod. Drug Discovery*. **2001**. 4, 49-50, 52.
38. Wender, P. A.; Handy, S.; Wright, D. L. Towards the ideal synthesis. *Chem. Ind.* **1997**. 765-774.
39. Zhao, Z.; Wang, J.; Mao, H. Q.; Leong, K. W. Polyphosphoesters in drug and gene delivery. *Adv. Drug Deliv. Rev.* **2003**. 55, 483-499.
40. Zhou, C. H.; Xia, X.; Lin, C. X.; Tong, D. S.; Beltramini, J. Catalytic conversion of lignocellulosic biomass to fine chemicals and fuels, *Chem. Soc. Rev.* **2011**. 40, 5588–5617.